SUSTAINABLE RURAL MICROGRID: ENGINEERING AND ECONOMICS

A Thesis

by

WILLIAM ROBERT HARRIS

Submitted to the Office of Graduate and Professional Studies of
Texas A&M University
in partial fulfillment of the requirements for the degree of

MASTER OF SCIENCE

Chair of Committee,	Mehrdad Ehsani
Committee Members,	Laszlo Kish
	Le Xie
	Douglas Allaire
Head of Department,	Miroslav M. Begovic

August 2017

Major Subject: Electrical Engineering

ABSTRACT

Traditional electrification strategies focused on centralized grid expansion are financially infeasible for extending electricity connections to millions of rural households in developing countries. Instead, estimates predict mini-utilities and off-grid approaches will need to provide electricity to at least 154 million households if universal electrification is to be reached by the target of 2030 set by the United Nations' Sustainable Energy for All Initiative. Additionally, the large populations within developing countries and predictions of future electricity consumption suggest that fossil fuel-based electrification strategies for these countries would vastly increase the volume of greenhouse gas (GHG) emissions per annum and should be avoided. Renewable technologies such as photovoltaic (PV) arrays, wind turbines, and biomass gasifiers provide sustainable energy alternatives. With the advent of such renewable technologies, DC microgrids are increasingly advantageous compared to AC systems in rural applications, predominantly due to the reduction of AC to DC power conversions and native DC tendency of loads. A holistic methodological approach to designing a mini-utility is described in this thesis, including technical, financial, and managerial considerations.

Microgrid architecture topologies are proposed in this thesis, including photovoltaic, biomass gasifier, and wind turbine generators as well as generator hybridization topologies. Rural systems have unique design challenges due to their consumers' low purchasing power, sparse population density, minimal power

consumption and tendency for slow growth. Sizing generators appropriately is paramount. In many cases, detailed renewable resource data may be unavailable, a condition taken into consideration by utilizing publicly available low-resolution global climate datasets from NASA for generator sizing purposes. Power converter topologies are also briefly discussed. As an example, a microgrid topology and business model is constructed for a model village case study using the methodology and architectures described in this thesis. The results of the case study highlight the limitations of minimizing net preset cost as an optimization objective and instead propose maximum average cost to period as an alternative metric for comparison. Additionally, longer loan periods are found to favor capital-intensive microgrid architecture, such as solar and wind technologies.

DEDICATION

To

My Loving Wife

ACKNOWLEDGEMENTS

I would like to thank my committee chair, Dr. Ehsani, and my committee members, Dr. Xie, Dr. Kish, and Dr. Allaire, for their guidance and support throughout the course of this research.

Thanks also go to my friends and colleagues and the department faculty and staff for making my time at Texas A&M University a great experience.

Finally, thanks to my parents for their encouragement and to my wife for her patience and love.

CONTRIBUTORS AND FUNDING SOURCES

Contributors

This work was supported by a thesis committee consisting of Professors Mehrdad Ehsani, Le Xie, and Laszlo Kish of the Department of Electrical and Computer Engineering and Professor Douglas Allaire of the Department of Mechanical Engineering.

All work conducted for the thesis was completed by the student, under the advisement of Dr. Mehrdad Ehsani of the Department of Electrical and Computer Engineering.

Funding Sources

This thesis was supported by the Thomas W. Powell ’62 and Powell Industries Inc. fellowship from the Department of Electrical and Computer Engineering.

TABLE OF CONTENTS

Page

Page

LIST OF FIGURES

Page

LIST OF TABLES

Page

1. INTRODUCTION

1.1 Rural Electrification

Globally, billions of people do not have access to electricity [1]. Most are concentrated in rural areas of developing countries. Access to electricity provides many benefits to communities in the developing world, including replacing hazardous methods of lighting such as kerosene and providing additional income from increased productivity. The traditional method of providing new electrical connections to communities has been through expansion of centralized grids. This method is economically unsustainable for some remote populations, typically involves increasing generation capacity of dispatchable generators that emit pollutants contributing to the greenhouse effect, and can require decades to extend infrastructure to rural regions. Decentralized microgrids utilizing renewable energy, however, can be installed relatively quickly and inexpensively to provide electricity to remote regions of the world.

In the context of rural electrification, microgrids are small electrical grid systems capable of generating and transmitting power to point of use. Microgrids can operate independently as an island or be connected to a larger network. Development of microgrids for use in rural electrification has predominantly been focused on metrics such as net present cost, loss of load probability, capital cost, and $C0_2$ emissions. While these metrics are relevant, demand-side design considerations are not typically included. Inclusion of design-side considerations requires a more detailed understanding of the business framework of rural mini-utilities and the needs of end-users.

The work presented provides a holistic approach to the methodology of designing mini-utility microgrids for applications in rural electrification. A financially viable mini-utility business framework is discussed and a renewable energy DC microgrid architecture is presented. Economic and technical models are described and implemented in MATLAB to determine optimal sizing of generators and energy storage in microgrid. A simulation case study of a model village was conducted to observe how the inclusion of debt can influence the optimal sizing of a microgrid and to examine effectiveness of net present cost when used as an economic optimization objective.

1.2 Thesis Overview

This thesis is organized into 7 sections. Section 1 outlines the research objectives and overview of the thesis. Section 2 provides background information discussing the current state of global electrification, motivation to increase the electrification rate, and methods of electrification as well as a brief literature review. Section 3 presents an outline of the business framework of rural mini-utility. The microgrid architecture is discussed in Section 4, including the microgrid topology and relevant power electronics. Section 5 presents the optimal sizing methodology utilizing worst month resource data. A model village case study is conducted in Section 6 and a conclusion of research results is presented in Section 7.

2. BACKGROUND

2.1 Current State of Global Electrification

According to the International Energy Agency (IEA), roughly 1.2 billion people did not have access to electricity in 2014 [2]. Another billion do not have access to reliable electricity [3]. Additionally, some of those individuals included categorized as having access to electricity are unable to utilize electricity due to economic barriers. In 2011 the United Nations began the first global initiative aimed specifically at eliminating energy poverty. The initiative, Sustainable Energy for All (SE4All), has three goals to achieve by 2030: ensuring universal access to modern energy services, doubling the renewable energy share of the global energy mix, and doubling the global rate of energy efficiency [1]. The human development index (HDI) is a tool used to assess the development of a country by quantifying and normalizing the average health, level of education, and gross national income per capita of the country. Access to electricity has been found to correlate strongly with improved human development index (HDI) over time [4, 5]. Even basic electrical lighting allows for increased productive hours in the day, increasing income levels as well as employment and educational opportunities [6-9]. Therefore, to alleviate poverty and improve quality of life, access to electricity is a necessity.

2.2 Trends and Projections of Global Electrification

Over 96% of those without access to electricity live in Sub-Saharan Africa or developing Asia. Most of those without electricity are in rural areas. While the urban electrification rate in developing countries is 92%, the rural rate is only 67%. The IEA

suggests that in order to meet the goals of SE4All annual energy access growth rates of 0.7% are necessary. In India and some of Southeast Asia the annual growth rate comes close to the target, but in Africa the progress is far slower. Overall, the annual growth rate has increased to 0.6% from the average growth rate between 2000 and 2010 around 0.2%. In some nations such as Myanmar, Angola, Ethiopia, Kenya, and Madagascar, population growth is outpacing access to electricity leading to lower electrification rates over time.

Table 1 Global energy electrification rates [2].

Electricity access in 2014 - Regional aggregates				
Region	Population without electricity	Electrification rate	Urban electrification rate	Rural electrification rate
	millions	%	%	%
Developing countries	1,185	79%	92%	67%
Africa	634	45%	71%	28%
North Africa	1	99%	100%	99%
Sub-Saharan Africa	632	35%	63%	19%
Developing Asia	512	86%	96%	79%
China	0	100%	100%	100%
India	244	81%	96%	74%
Latin America	22	95%	98%	85%
Middle East	18	92%	98%	78%
Transition economies & OECD	1	100%	100%	100%
WORLD	1,186	84%	95%	71%

Consumption of energy has historically been concentrated in a few industrialized nations. Increasingly, however, developing nations are making rapid advancements in energy consumption as their national economy and quality of living improve. In 1974, the countries composing the Organisation for Economic Co-operation and Development (OECD), roughly representing the developed world, consumed 60% of the world's

energy. By 2014, their share of the global energy consumption had declined to 38% and it continues to fall as more low and middle income nations expand their energy infrastructure [10]. Efforts in developing nations to achieve universal electrification for their citizenry will continue to increase the share of global energy consumption by non-OECD nations and the overall global energy consumption. Global consumption of electricity reached 24.1 PWh in 2015 and if the trend from the last decade of growth continues, global consumption is expected to grow 48% between 2015 and 2035 [11]. From 2005 to 2015, the electricity generated by OECD member nations increased by 2%. By comparison, the electricity generated by non-OECD nations increased by 71% [11]. The trend of nearly stagnant growth in energy consumption for the developed world and rapid growth by the rest of the world is expected to continue and become even more pronounced over the next 50 years.

2.3 Fossil Fuels

Combustion of fossil fuels produces both gases and particulates that are hazardous directly or indirectly to humans. Some emissions, such as CO_2, are greenhouse gases (GHG) that trap heat in the earth's atmosphere in a process known as the greenhouse effect. Combustion of kerosene for lighting and cooking in the developing world emits a GHG known as black carbon, which has been found to cause significant impact to local warming as shown in Fig. 1. Additionally, kerosene is known to produce fine particulates, carbon monoxide (CO), nitric oxides (NO_x), and sulfur dioxide (SO_2), which can result in numerous health conditions such as impairment to lung function, tuberculosis, asthma, and cancer [12]. Sulfur dioxide can also mix with

water in the upper atmosphere and turn into sulfuric acid, known as ‘acid rain’ when it falls to earth.

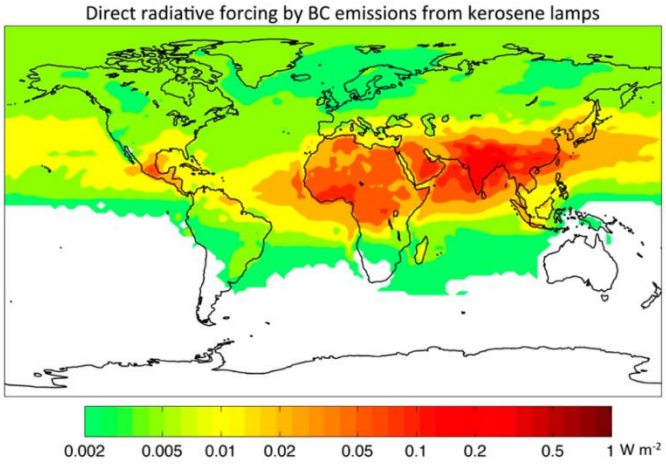

Fig. 1 Contributions of black carbon emissions from simple wick kerosene lamps [13]

In matured countries such as the US, applications of fossil fuels are usually more inexpensive than replacement renewable technologies. In the developing world, however, replacement of kerosene with LEDs for lighting can provide brighter light at a cheaper cost with less GHG emissions.

Additionally, fossil fuels resources are finite and fungible, leading to price fluctuations of fuel prices. As energy consumption in the developing world increases, fossil fuel price volatility will continue to grow. Fossil fuels are necessary for transportation, but renewable alternatives are more attractive in the long-term for applications such as electricity generation [14]. As Fig. 2 shows, it is more important with regards to climate change to focus on developing carbon-neutral, sustainable energy infrastructure for the developing world than to replace existing fossil fuel-based infrastructure in the developed world.

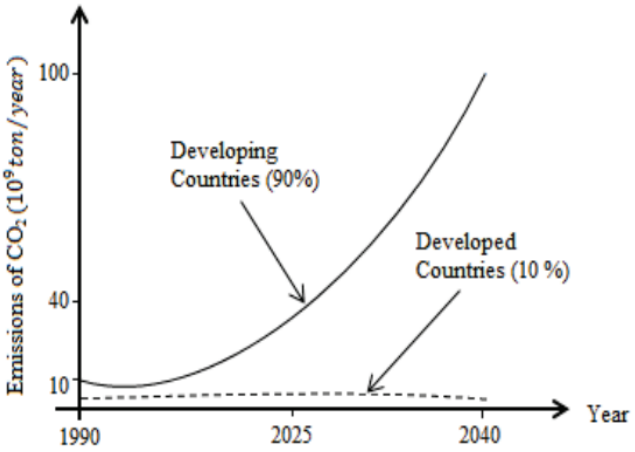

Fig. 2 Projected CO2 emissions from developed and developing countries [15]

2.4 Concept of Sustainability

A system can be described as sustainable if the system is able to continue indefinitely without depleting a finite resource. Rural electrification cannot be accomplished if the solutions are short-sighted. Many organizations are structured in a way that that provides unsustainable electrification technologies and then no additional assistance when the system proves inviable. As an example, subsequent to the fall of the Taliban in Afghanistan, some donors gave diesel generators to communities as a solution to immediate energy needs. This costly solution had several long term flaws; most notably the cost of electricity became tied to a volatile fossil fuel supply and pollution. Purchasing the diesel generators ultimately cost the community much more than purchasing other technologies that require less operating cost [16]. Sustainable development has been described as having five pillars: environmental, social, economic, technical and institutional [16, 17].

In many publications focused on the development of rural microgrid systems the economic, technical and sometimes environmental pillars are given priority, but the social and institutional pillars are not accounted for [18-25]. Instead a rounded approach is necessary that takes into account long-term sustainability on all fronts. All five pillars of sustainability development should inform the technical design. An ideal sustainable solution should have all the qualities described in Table 2.

Table 2 Sustainable Energy Requirements [14]

Terminology	***Definition***
Adequate	No energy limits on economic development and prosperity.
Ecological	Environmentally acceptable
Economical	Reasonable capital & production cost, market compatible.
Realizable	Starting with the present infrastructure, smooth transition to future technologies.
Global	Producible in the United States and elsewhere, eliminating international "haves and have-nots".
Publicly Acceptable	Compatible with the public sense of risk, aesthetics, ethics, etc.
Unifying	Compatible with the sense of world economic equity and world community.
Robust	Not prone to technical failures, not maintenance intensive, no single-point failures.
Secure	Not concentrated, volatile, vulnerable to terrorism.

2.5 Rural Electrification

The central concept of rural electrification is to replace traditional fuels such as kerosene and burning raw biomass with cleaner and cheaper electricity. This reduces the amount of money individuals must spend on energy every month and also reduces the pollution added to the atmosphere which has had both global and local consequences. Benefits of rural electrification also includes increased employment opportunities, increased harvest yields from agriculture, reduction of deforestation, and increased education opportunities [6]. To effectively supplant traditional energy spending, the cost

of electricity must allow end-users to spend less than they are already. Many individuals who could benefit from electrification are skeptical and will not utilize electrical services unless there is a cost savings. For communities spending less than $1.25 per month on traditional energy sources, this condition makes electrification with current technology pricing virtually impossible [26]. Basic lighting and small device charging can be provided by different levels of approach including rechargeable lanterns, small solar kits, and modern electrification strategies such as solar home systems (SHS), microgrids, and grid extension. In general, rechargeable lanterns, small solar kits, and solar home systems are suitable for initial access to electricity at low power demand levels, but as demand increases, all communities will need systems with larger power capacities such as SHS, grid extension and microgrids.

The rapid widespread adoption of cell phones in the developing world may demonstrate the best method of penetrating rural low and middle income regions of the world [7]. The spread of landline phones was sluggish due to the high capital cost of copper and the long distances involved. A paradigm shift occurred from the invention of cell phones. Mobile phones provided an obvious benefit towards communication at a reasonable price to the consumer and much less capital cost to businesses providing the technology. As a result, by 2014 more than 80% of adults in countries such as South Africa, Ghana, and Kenya owned a cellphone, while less than 5% had a landline [27]. The comparison to rural electrification points towards decentralized grids and home systems that are able to rapidly spread by foregoing the costly transmission lines necessary for traditional grid expansion-based methods of electrification. Decentralized

rural electrification will be the only way to reach over 116 million people [3], but it also holds the possibility to become ubiquitous even in areas where extension of centralized grids is feasible if self-sustaining, financially viable business models and technology are developed.

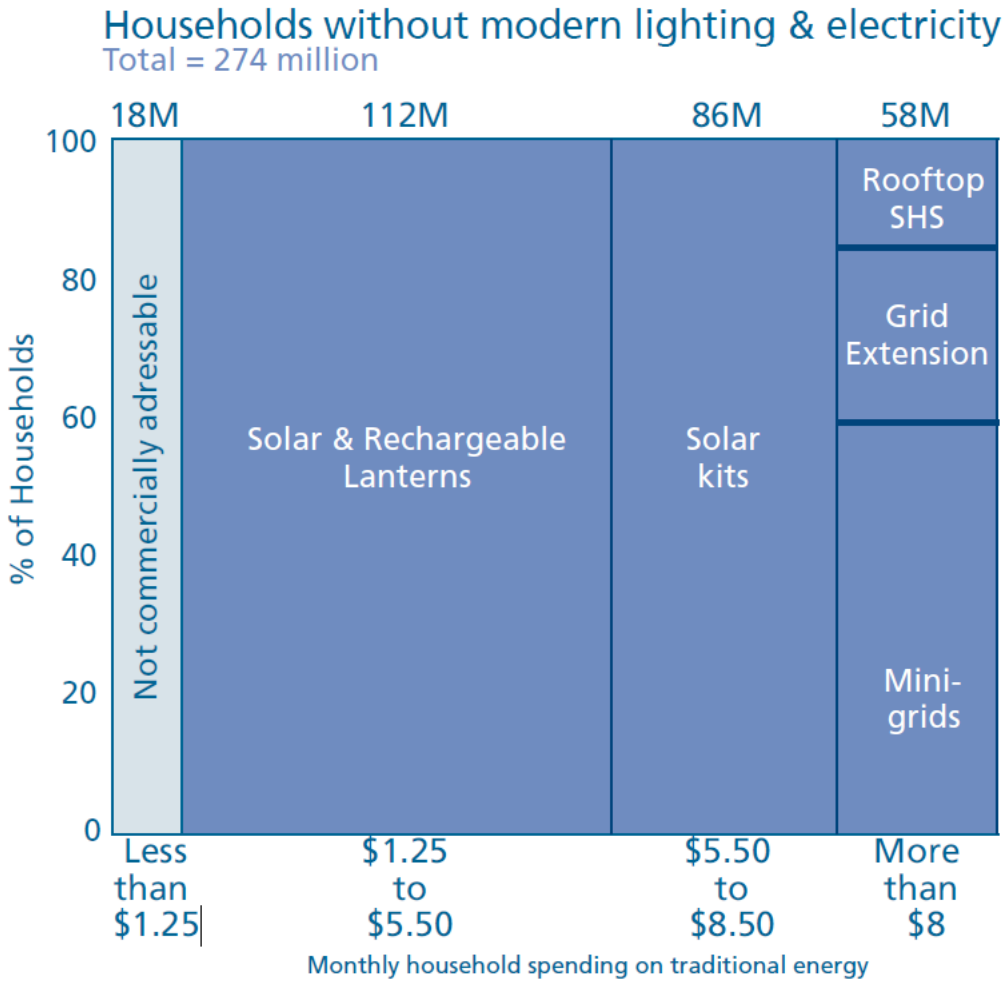

Fig. 3. Estimated breakdown of households without modern lighting and electricity requiring off-grid solutions [26]

2.6 Methods of Rural Electrification

2.6.1 Extension of Centralized Grids

Both national and private extensions of centralized grids are traditionally thought of as the method of providing electricity access to communities, however, adding additional generation and transmission lines is extremely capital and time intensive and is not a feasible solution for many regions. While some nations such as China and Brazil have been very successful in increasing their electrification rate to rural populations by extending national grids, the expenses have been very high per capita and frequently financially inviable without state subsidy [28]. Estimates for extension of the grid to the Western and Northwestern regions of China are between $5000-$12,000 per km and the unsubsidized price of electricity would be $3.32 per kWh [29]. The first stage of Brazil's "Luz para Todos" initiative which aimed at increasing the electrification rate of the country cost $854 million and provided 567,000 connections, at a cost per connection of $1,487 per connection [30]. This cost is extremely high per connection and many other developing countries do not have the ability to subsidize or otherwise fund the high capital requirements.

2.6.2 Microgrid

There is some ongoing confusion over what the precise definition of the term 'microgrid'. Microgrids are typically defined as having distributed resources and loads and the ability for grid connection or island operation. The use of the term is closely related to smart grids and distributed generation applications in the matured power grids of the developed world, especially in the US. Nevertheless, microgrid has also been used

to refer to islanded grids unconnected to any other centralized grid with no intention for future grid connection. For the purposes of this thesis, microgrid will refer to a grid that features connections between multiple homes and has a higher transmission voltage than the household utilization voltage, whereas off-grid will refer to a system sized for a single home with no higher voltage used for transmission. Additionally microgrids may have a single point of generation rather than a distributed generation topology.

As a method of providing rural electrification, microgrids offer several advantages. Foremost, microgrids are more inexpensive to install per connection compared to central grid expansion. The reduced system size of microgrids significantly reduces the capital cost, as well as operations and maintenance costs. Microgrids also operate at much lower voltages than are necessary for traditional centralized grids, allowing for less expensive and smaller transmission and distribution installations without the need for substations and large high voltage transmission towers. In rural systems, reliability of electricity, while important, is also of reduced importance in favor of making the mini-utility service available for as many villagers as possible. In communities without an existing structure for electricity supply, renewable energy systems are better able to supply electricity [31]. Microgrids can also generate local employment and become accepted as a valued asset of the community.

2.6.3 Off-grid

Off-grid systems are systems that provide electricity for a single building or cluster of buildings, but are otherwise unconnected to other generators or loads. Most off-grid systems are roof-mounted or ground-mounted PV panels combined with battery

storage to provide enough electricity for small loads. Home systems are suitable under conditions where sparse population density, major geographic obstacles, or other conditions make even the low voltage transmission lines of microgrids economically infeasible. Home systems typically provide limited power and can be more expensive to increase the power capacity of the system per household than microgrids.

2.7 Common End-Uses of Electricity

The most basic use for electricity is for lighting, however, if this is the only electrical application then a small solar lamp may be satisfactory. The benefit of a mini-utility is that end-users can add to their electrically-power devices and appliances over time as they gain income. In addition to basic lighting, charging small devices such as cell phones is a nearly universal need. Even in communities where electricity access is uncommon, many individuals still have cell phones. These individuals will travel a dozen miles to charge their phone for a high fee. The ability to charge mobile phones and other small electronics within their own home is a major benefit as it saves time and money. Because a large majority of households without electricity are in regions within 30 degrees of the equator fans are needed for cooling in many areas of the world. Depending on the sort of work that is available in the area, some labor-saving devices may be necessary as well. This can include irrigation pumps and grain threshers. Income-generating applications of electricity are highly important for the survival of the mini-grid and also for the community. They increase the income for the community and also make the community more dependent upon the mini-grid. This can assist significantly in raising communities out of poverty.

2.8 Renewable Generation

2.8.1 Solar

PV technology generates direct current (DC) by generating proportional current to incidental photon intensity through the photoelectric effect. A simple circuit model is shown in Fig. 4.

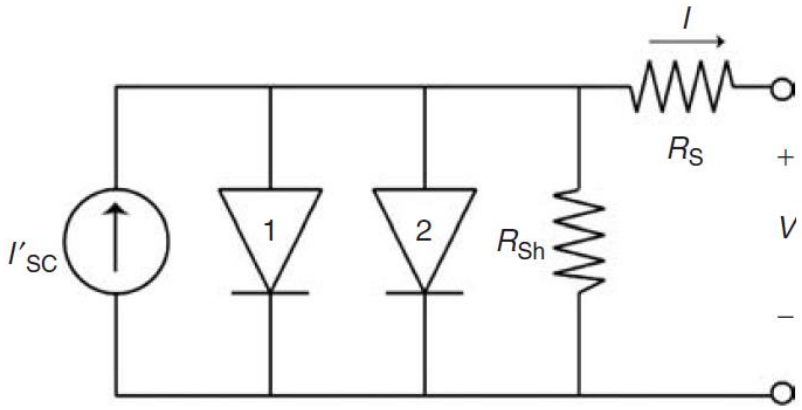

Fig. 4 Simple PV circuit model [32]

The current produced by a solar cell can be described by equation (1).

$$I = I_{SC} - I_{o1}\left(e^{(V+IR_s)/V_T} - 1\right) - I_{o2}\left(e^{(V+IR_s)/(2V_T)} - 1\right) - \frac{(V + IR_s)}{R_{Sh}} \qquad (1)$$

where

I = Output current

V = Output voltage

I_{SC} = Short circuit current without parasitic resistances

I_{o1} = Diode 1 saturation current

I_{o2} = Diode 2 saturation current

V_T = Thermal voltage

R_S = Series resistance

R_{SH} = Shunt resistance

The current-voltage characteristic of a typical PV module is shown in Fig. 2.3. Of special importance is the maximum power point, where the power output is optimized by purposely varying the apparent output impedance of the DC-DC converter. Under different solar insolation conditions and junction cell temperatures, the maximum power point will shift due to the proportional relationship the solar module output current has with input irradiance. At the maximum power point,

$$V = V_{MP}$$

and

$$I = I_{MP}.$$

The maximum power point can be found for any instantaneous current-voltage characteristic by solving the following equation:

$$\left.\frac{\partial P}{\partial V}\right]_{V=V_{MP}} = \left.\frac{\partial (IV)}{\partial V}\right]_{V=V_{MP}} = \left.[I + V\frac{\partial I}{\partial V}]\right]_{V=V_{MP}} = 0 \qquad (2)$$

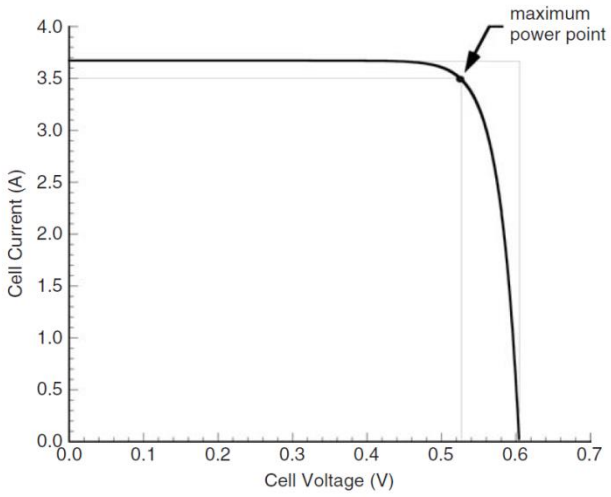

Fig. 5 Typical current-voltage characteristic of a silicon solar cell

PV modules' nominal power output is measured under Standard Testing Conditions (STC), where the reference spectrum is global, irradiance is 1 kW m^{-2} and the cell temperature is 25 °C. This is referred to as their Watt-peaking output, or derated output. Due to thermal voltage effects in in equation (1), realistic power output will be different due to the temperature of the solar cells. Irradiance or insolation refers to the quantity of solar power and is measured in watts per meter squared. Global horizontal irradiance is the amount of irradiance striking a plane horizontal to the surface of the earth. It is composed of direct horizontal irradiance and diffused horizontal irradiance.

Prices of PV modules have decreased significantly in the last 30 years, with a continuing downward trend expected as hardware price decreases. Recent pricing trends are shown in Fig. 6. This is advantageous for rural electrification purposes because solar

panels are now inexpensive enough to provide economically feasible remote power generation.

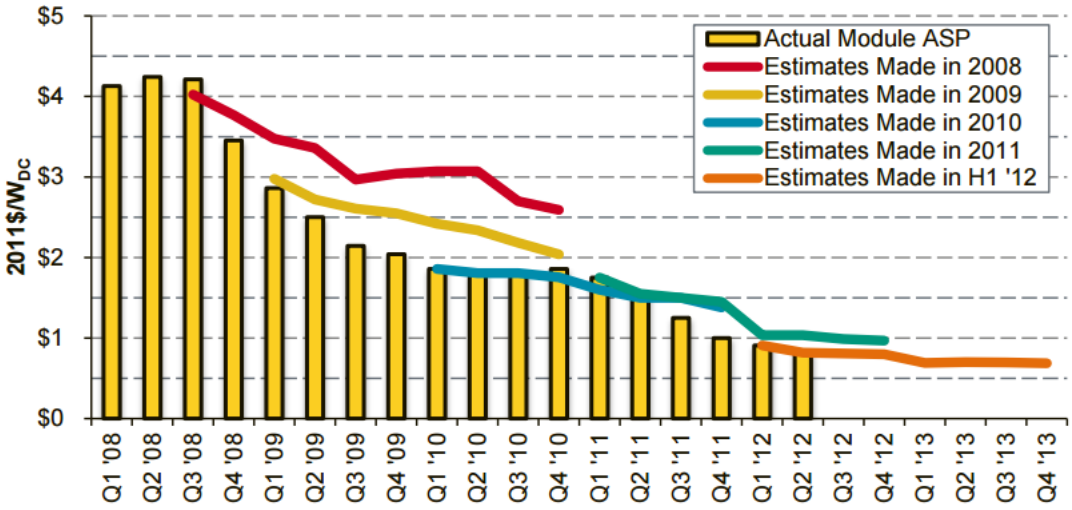

Fig. 6 Average module selling prices, predictions and actual [33].

2.8.2 Wind

Small scale wind turbines have rotor diameters between 3 and 10 meters and a standard power rating between 1.4-25 kW [34]. While both vertical axis wind turbines and horizontal wind axis turbines are on the market, a majority of small scale wind turbines are horizontal axis. Most small wind turbines are single phase AC generators, which when connected to an AC system, must be first converted to DC and then back to AC in order to maximize power and synchronize frequency. Integration into a DC system, by comparison, requires one fewer power conversion between DC and AC, making integration into DC systems more efficient than AC systems. Additionally, in a DC system a self-exciting DC generator or permanent magnet brushless DC generator

can be used the wind turbine to eliminate the need rectification of an AC signal at all. This approach has been explored in theory in literature [35, 36], but requires further research.

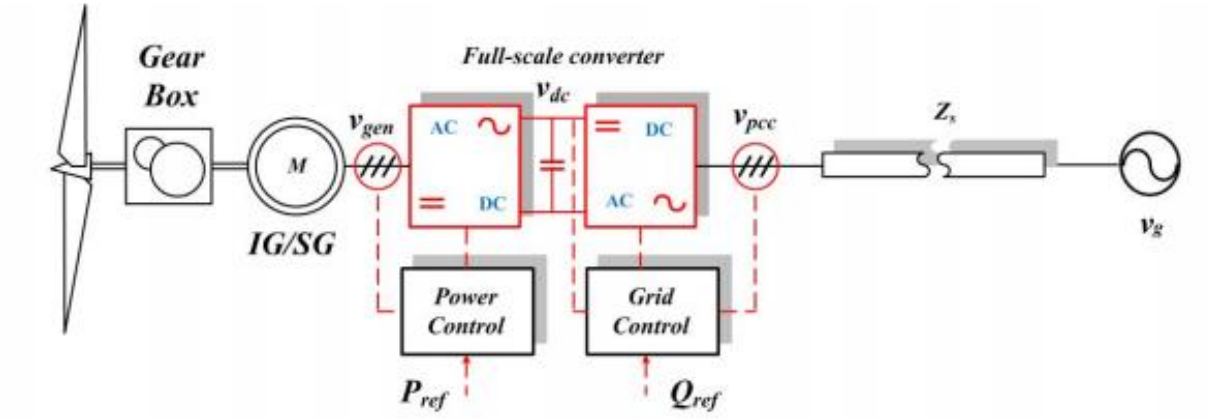

Fig. 7 Simplified diagram of wind turbine integration into AC grid [37].

2.8.3 Biomass

Biomass gasification produces a combustible mixture of gases known as producer gas [38] is created from raw biomass, such as corn cobs, rice husks, coconut shells, etc.. Burning biomass directly releases several damaging pollutants into the atmosphere, however, through the gasification process, the final combustion can emit less pollution. In regions with large agricultural activity, biomass gasifiers can be easily fed with renewable fuel sources that have minimal price volatility compared to fossil fuels and create a net reduction in pollutant emissions. Availability of biomass resources can experience seasonal volatility but can be counter-balanced by using diverse biomass sources.

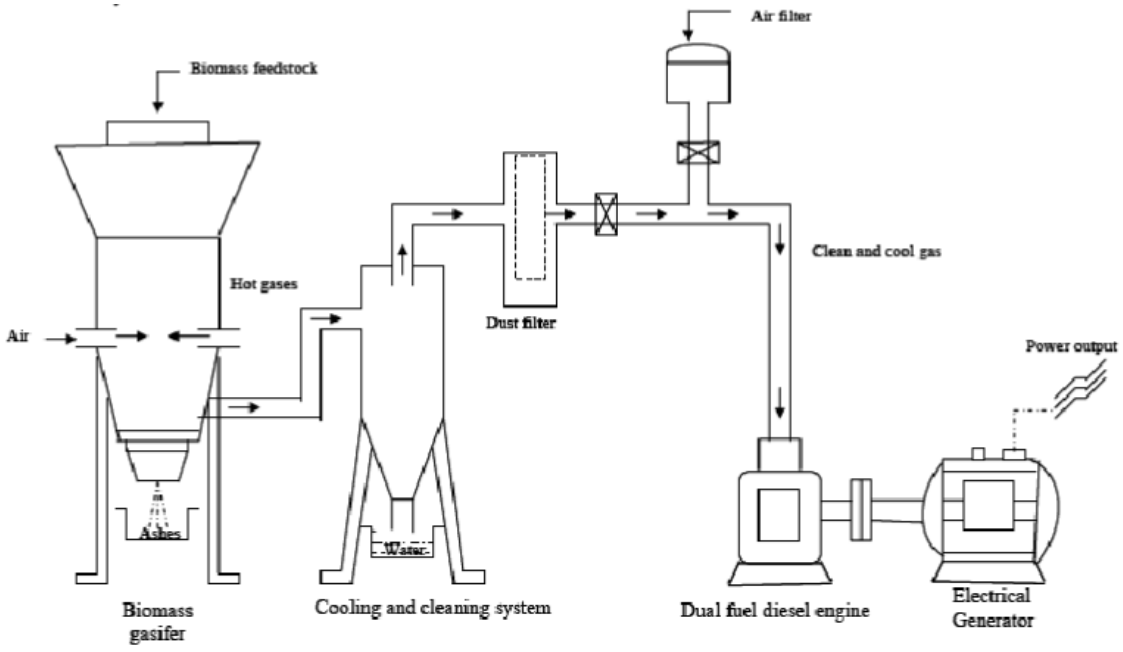

Fig. 8 Biomass gasifier diagram.

2.9 AC and DC Microgrids

The "War of the Currents" over a century ago established AC systems as the standard in power distribution, predominantly because of the simple ease of changing voltages using transformers for long-distance distribution [39]. Despite the ascension of AC systems to become the standard in power distribution, DC systems have recently become increasingly common in an expanding number of applications such as electric vehicles, shipboard systems, datacenters, and telecommunication systems [40]. High voltage direct current (HVDC) transmission has also become more commonly used in applications such as linking asynchronous AC grids and bulk power transmission over

long distances [41]. While established AC grids are in no danger of being replaced by DC grids, distributed generation made possible by solar panels has made the concept of hybrid AC and DC systems conceivable in developed countries [42]. Recent advancements in power electronics have allowed DC microgrids to become possible solutions that can rival the cost of AC systems, specifically the developments with regards to cheap and efficient DC-DC converters capable of competing with transformers. DC currents generated from PV modules can more efficiently deliver power to loads in DC microgrids because DC-DC conversion is more efficient than an inverting the current. In addition to native DC generators such as PV, both intermittent and dispatchable AC generators are able to operate more efficiently in DC systems because they can produce the frequency of the optimal operation point of the generator rather than the frequency of the AC system. Many loads are now natively DC, requiring a power conversion for AC systems from AC to DC that involves power losses and loss of reliability.

Additionally, DC systems' power electronics can operate as a firewall to prevent disturbances from affecting other sections of the network. In cases where the DC microgrid is grid-connected, the power electronics can prevent external disturbances on the national grid from destabilizing the microgrid and similarly prevent microgrid disturbances from affecting the national grid.

The major benefit for AC systems in terms of safety is the zero-point crossing of current that allows a temporary period of time at low current for an individual in contact with live wires to break free. The safety threshold for DC voltages below 50 VDC are

considered safe for human contact up to three seconds [43]. The standard distribution voltage for telecom sites is 48 VDC as the distribution voltage and this voltage shows promise as a new international standard [44, 45]. Lighting and appliances designed for 48 VDC are already on the market, allowing for immediate implementation in rural DC microgrids.

A DC system can pass more power through the same sized cable than an AC system which reduces capital costs for the cable. DC has a power factor of 1 and does not have reactive power losses that reduce the apparent power of AC systems.

$$P_{AC} = i_{rms} v_{rms} \tag{3}$$

$$v_{rms} = \frac{V_{peak}}{\sqrt{2}} \tag{4}$$

$$P_{DC} = i_{rms} v_{peak} = \sqrt{2} i_{rms} v_{rms} = \sqrt{2} P_{AC} \tag{5}$$

Most importantly for applications in the developing world where energy spending is less than $10 a month, DC microgrids are cheaper for end-users. Indian homes with loads of less than 125 W were found to have monthly cost benefits of over $5.90 when a DC microgrid and AC microgrid were compared [7]. The DC microgrid was found to be more energy efficient, using nearly 64% less energy daily than a comparable AC microgrid.

2.10 Financial Viability

In order for investments into rural electrification to be effective, it is essential that rural mini-utilities are self-sustaining independent of subsidy or grants. Policies may or may not be in the favor of renewable energy or decentralized grids, but even in the

absence of subsidy, mini-utilities must be able to attain financial viability to continue to operate. Different locations have different resources so some are more financially viable than others. Those that are more financially viable should have priority. Those without financial viability should be the focus of humanitarian donations of solar lighting equipment. Subsidies can negatively impact market conditions and consumer willingness to pay for electrical services. For example, if an organization gives free equipment or free electrical connections out to some communities, neighboring communities will be less willing to pay for access to electricity. Both subsidy and humanitarian donations need to be carefully calibrated or they can severely inhibit the local market for electricity access.

Some nations such as India provide subsidies for kerosene, causing significant issues in the market competitiveness of renewable technologies which would otherwise be competitive while not causing the fire and health risks associated with traditional fuels [46]. There are no associated risks with replacing kerosene used for lighting purposes with electrical lighting.

2.11 Problem Statement

This thesis seeks to design a mini-utility microgrid architecture and business model framework to provide first-time connection to electricity from renewable energy to rural, impoverished populations in developing countries. The envisioned business model framework overview will be explained, including financing and socio-economic impact. The microgrid architecture will be dealt with in two steps. The first step is to describe the features of the microgrid architecture and the second step is to describe the

methodology of optimally sizing the generators and energy storage appropriately. Sizing and selection of generator types should be achieved in conditions where minimal local renewable resource information is available as is typical for remote, rural communities.

3. BUSINESS MODEL FRAMEWORK

A mini-utility operates a microgrid and collects payments from end-users in the community, all in a single, compact organization. There are many ways to structure a rural mini-utility depending upon site-specific parameters such as villager willingness to pay for electricity and relevant local policy. This section introduces a proposed business framework.

3.1 Operators

Mini-utility operators should ideally be locals, either entrepreneurs or a co-op, who provide 10% of the capital investment needed for the project. The entrepreneur or co-op would seek to pay off the loan to receive full ownership of the mini-utility. Locals are more likely to be able to navigate village politics and more likely to be trusted by potential customers. Other positions will also need to be filled on the local level including technicians and payment collectors, which adds to the integration of the mini-utility into the community. Community involvement and feelings of ownership in the technology are integral to mini-utility success, especially in regions where individuals are skeptical or suspicious about electricity [17, 26, 47-49].

3.2 Higher-Level Framework

Finding sources of capital is the greatest obstacle for rural electrification projects [50]. For this thesis, it is proposed that a larger regional or international organization helps facilitate local mini-utility startups by providing opportunities for loans. This organization would probably need to have predominantly humanitarian goals, as the rate of return on mini-utilities is frequently under 10%. The organization would be able to

provide revolving funds to underwrite the loan for the capital needed to create the mini-utility. After the funds are paid back at a small interest rate, the same money can be used to provide financing for other electrification projects. This model still puts pressure on the project to be financially viable while providing the funding for the mini-utility that can be difficult to find elsewhere. This organization can alternatively underwrite loans from local banks to further stimulate the local economy. Capital can otherwise be sourced from international financial institutions, non-governmental organizations, and private investors. A single entrepreneur or co-op could continue to grow the mini-utility and start other mini-utilities in the area. Multiple mini-utilities under a single owner could be sold to larger utilities or other interested parties. Ideally, a franchise model would be best, where a central company assists local entrepreneurs with launching mini-utilities in their villages and takes a percentage of profits. One company, Husk Power Systems, has begun the process of developing a franchise framework based on the design, build, and maintain (DBM) model, where mini-utilities design, construction, and maintenance would be done by the company, while local entrepreneurs own and operate the system. [26]. This model combines the benefits of a larger organization, such as relationships with financial institutions and manufacturers and experience with microgrid construction and operation, with the benefits of local knowledge and influence [47].

3.3 Capital Structure

Types of capital can be divided into three categories: grants, debt, and equity. The term grant is used here to describe capital sourcing without financial return on

investment. Examples of grants include a donation of funds from a non-governmental organization (NGO) or a subsidy of $100 per kW from the regional government on a generator installation. Debt, by comparison, is a loan of money which requires a return on investment for the lender, in this case, principal plus interest. Loans can have a range of payment periods and interest rates, based on perceived risk of the investment. Assets can be included in a loan as collateral to mitigate risk. Equity capital carries an expectation of a return on the investment for shareholders.

In the case of rural electrification, debt is generally preferable to equity because it has a limited payback period allowing ownership to revert back to the entrepreneurs. For complete fully privatized financial viability of the business model, grants and subsidies should be unnecessary for the project.

3.4 Payment Schemes

Rural electrification requires payment schemes appropriate for impoverished customers. Traditional utility payment schemes where consumers pay for their previous month's energy usage at a flat cost per kWh is not an effective payment scheme for rural communities because of the volatility of income in many regions. Instead other payment schemes such as pre-paid meters are better suited [26, 51]. The prepaid scheme is effective because it counters income volatility by allowing consumer to pay for electricity only when they are able to. This way customers cannot develop outstanding debts to the mini-utility, which is a frequent cause of theft and restricting future usage of electricity, and the utility is able to both generate more revenue and reduce power used without payment. Another alternative is a flat monthly fee for connection and then

residents can use as much power as they need to. Tiered pricing can also be implemented to charge commercial connections a higher price than residential. An upfront fee for each connection can establish an investment into the service for customers, but can also create an additional economic barrier to customers preventing them from utilizing the electricity.

4. MICROGRID ARCHITECTURE

4.1 Microgrid Topologies

The general outline for microgrid design can be found in Fig. 9. Generators are connected to a DC bus through power electronics and a step down DC-DC converter is used to connect loads to the DC bus. All components of the microgrid are therefore decoupled, allowing for simple fault isolation through power electronics controllers. Here three candidate technologies are proposed as generators: PV, wind turbine, and biomass gasifiers. Optimal sizing described in Section 5 can be used to determine the best topology for a site, but options can include a single generator technology or hybridizations of multiple generators. The proposed DC bus is 300 VDC, while the utilization voltage for household loads is 48 VDC, though either voltage could be designed differently. On the load side, step-down converters at nodes provide electricity for multiple homes.

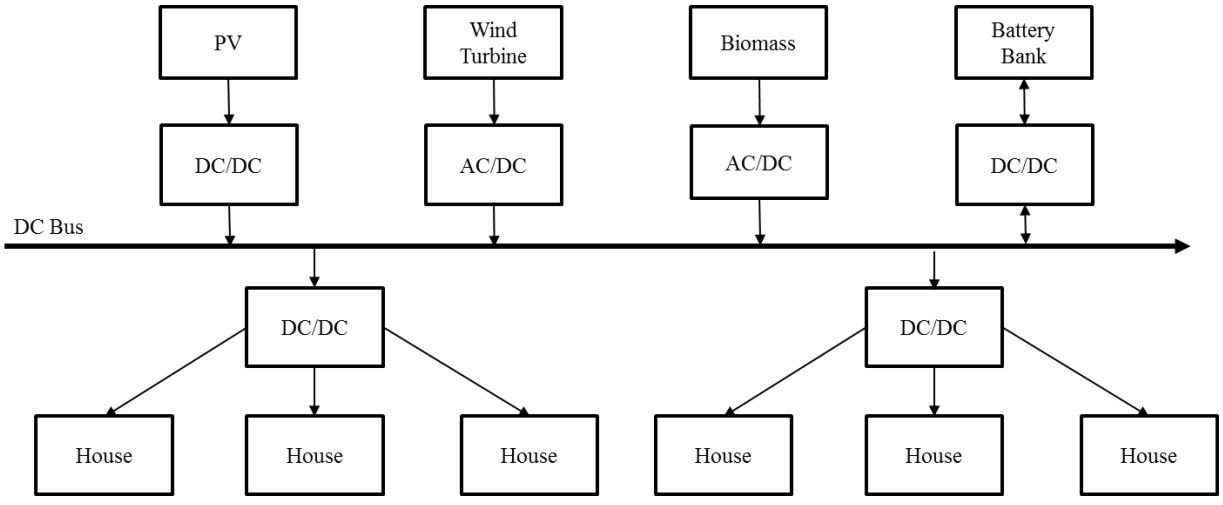

Fig. 9 Microgrid architecture overview.

4.2 Transmission

One of the major advantages of DC microgrids is that more power can be passed through a conductor at given voltage than an AC system. Conductor gauge is sized by first determining the maximum amount of current that is expected during normal operation and the ampacity is oversized by at least 125% [52]. A thicker insulated cable can be used to distribute power over greater distances, as the greater cross sectional area reduces the resistance of the metal, and has the added advantage of being versatile enough to be buried underground or strung overhead without being a serious danger. When being strung overhead, bamboo can be used as poles to prop up the cable. Bamboo poles are inexpensive and easy to replace.

4.3 Power Electronics

4.3.1 Voltage Step Up

In the case of PV, a high step up DC/DC converter is necessary to boost the output of the PV panels to the DC distribution voltage. The high step-up converter is needed to reduce transmission losses. One such high step-up DC/DC converter is the Z-source DC/DC converter with flyback and voltage multiplier shown in Fig. 10 [53]. This high step up dc-dc converter builds upon the Z-source converter, which can attain a higher voltage gain for the same duty cycle as a conventional boost converter, increasing the efficiency of the converter for high step-up applications [54].

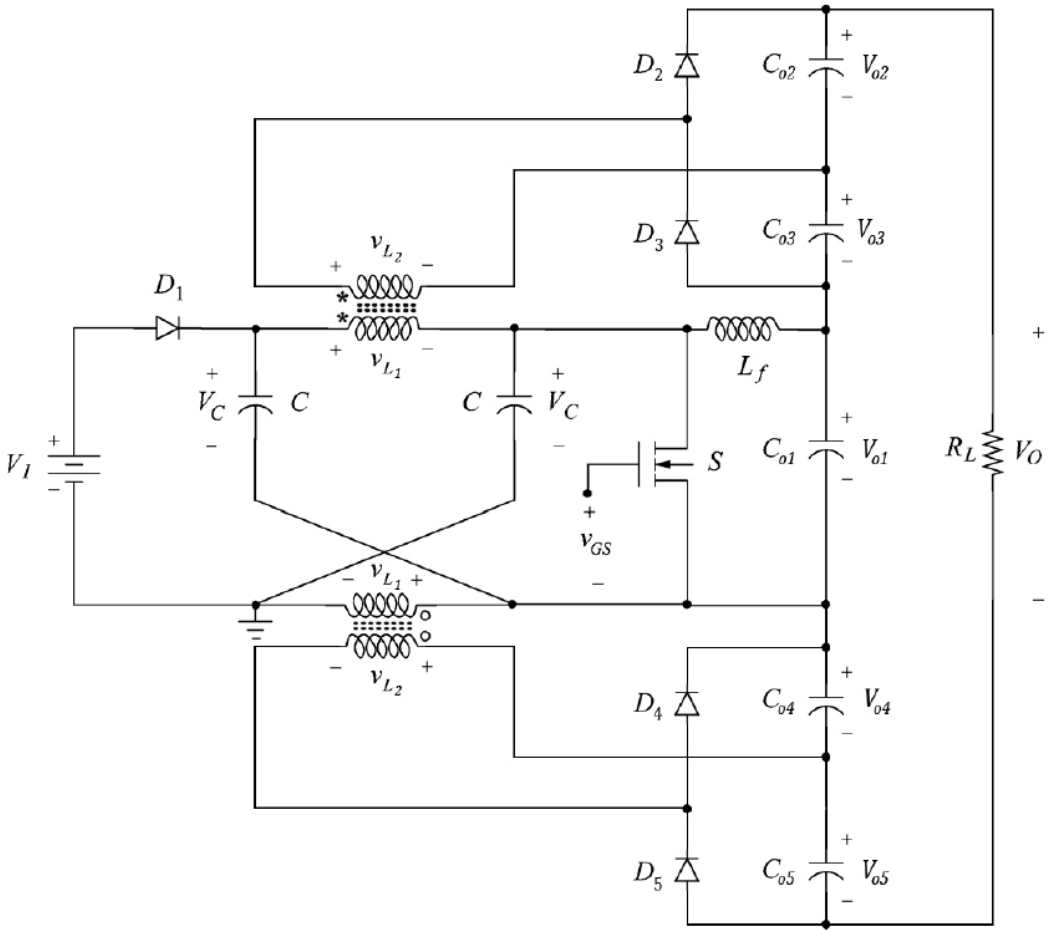

Fig. 10 Topology of Z-source DC-DC converter with flyback and voltage multiplier [53]

Semiconductor devices are assumed to be ideal and the converter is operating in continuous current mode, CCM. The controlled via pulse width modulation or PWM. The duty ratio is defined by equation (6).

$$D = \frac{T_{on}}{T_s} \tag{6}$$

where

T_{on} = Pulse width

T_s = Switching period of PWM signal

There are two operating modes of this DC-DC converter. Coupled inductors turn ratio is defined by equation (7).

$$n = \frac{N_s}{N_p} \tag{7}$$

where

n = Turn ratio

N_p = Number of turns of the primary inductor

N_s = Number of turns of the secondary inductor

The turn ratio of the twin sets of coupled inductors in this converter, L_1 and L_2, is given in equation (53) such that the voltage across the L_2 inductors is n times the voltage across L_1.

$$n = \frac{n_2}{n_1} \tag{8}$$

where

n = Turn ratio

n_1 = Number of turns for L_1 inductors

n_2 = Number of turns for L_2 inductors

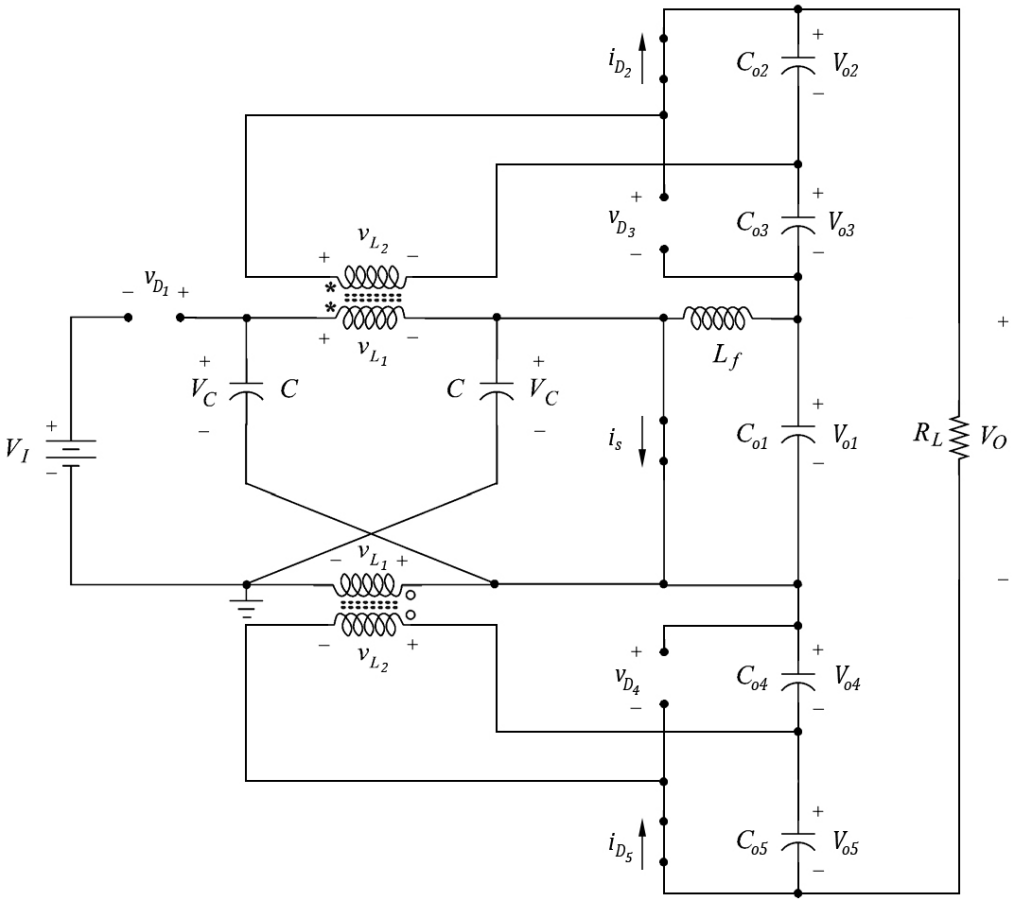

Fig. 11 Equivalent circuit during T_{on} when switch S is on [53]

Operation mode 1, shown in Fig. 11, takes place during period T_{on}, from time 0 to DT_s. During this period the active switch S is on and the input diode D_1 is off. The states of the input diode and active switch are always complementary in nature. The capacitor voltage, V_C, is applied across the L_1 inductors, causing a constant, linear increase in current from the L_1 inductors. A voltage proportional to the voltage across the L_1 inductors is excited in the L_2 inductors, causing the D_2 and D_5 diodes to turn on while the diodes D_3 and D_4 remain off, charging capacitors C_{o2} and C_{o5}. The filter inductor L_f is negative in operation mode 1, causing current to decrease linearly and energy to be lost

from the inductor. Voltages equations for operation mode 1 are described by equations (15) - (14).

$$V_{L1} = V_C, \tag{9}$$

$$V_{L2} = n * V_{L1} \tag{10}$$

$$V_{o2} = V_{o5} = V_{L2} = n * V_C \tag{11}$$

$$V_{D1} = 2V_C - V_I \tag{12}$$

$$V_{D3} = V_{o2} + V_{o3} \tag{13}$$

$$V_{D4} = V_{o4} + V_{o5} \tag{14}$$

Operation mode 2, shown in Fig. 12, takes place during period T_{off}, from time DT to T(1-D). During this period the active switch S is off, increasing the voltage across the switch until the input diode D_1 is turned on. During this mode, the *C* capacitors charge while the L_1 inductors discharge their stored energy from mode 1. A negative voltage n times the voltage of the L_1 inductors is excited in the L_2 inductors, causing the D_3 and D_4 diodes to turn on while the diodes D_2 and D_5 are off, charging capacitors C_{o3} and C_{o4}. Voltages equations for operation mode 2 are described by equations (15) - (21).

$$V_{L1} = V_I - V_C \tag{15}$$

$$V_{L2} = n * (V_I - V_C) \tag{16}$$

$$V_{o3} = V_{o4} = -V_{L2} = n * (V_C - V_I) \tag{17}$$

$$V_s = 2V_C - V_I \tag{18}$$

$$V_{D2} = V_{o2} + V_{o3} \tag{19}$$

$$V_{D5} = V_{o4} + V_{o5} \tag{20}$$

$$V_{Lf} = 2V_C - V_I - V_{o1} \tag{21}$$

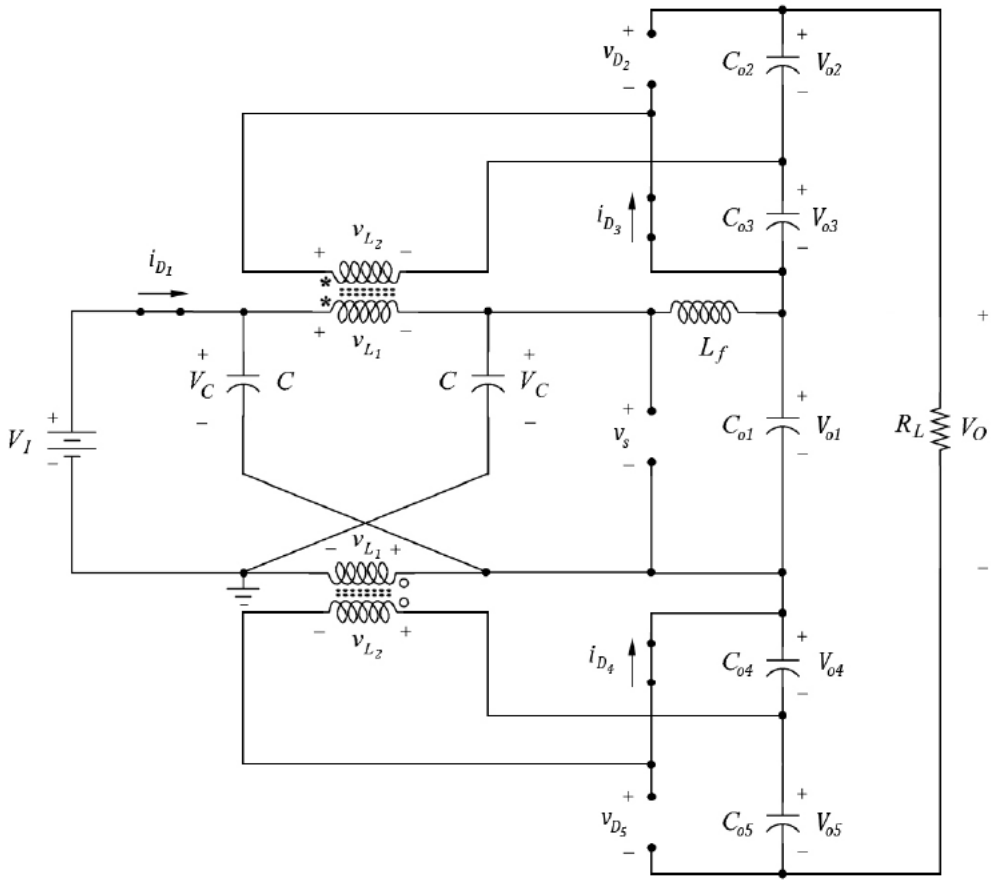

Fig. 12 Equivalent circuit during T_{off} when switch S is off [53]

Voltage gain of the converter is given in equation (22).

$$G_V = \frac{V_O}{V_I} = \frac{(2n+1) - D}{1 - 2D} \tag{22}$$

Current gain of the converter is given in equation (22).

$$G_I = \frac{V_O}{V_I} = \frac{(2n+1) - D}{1 - 2D} \tag{23}$$

4.3.2 Voltage Step Down

Step down DC-DC converters are necessary to reduce the transmission voltage to the utilization voltage of households. This can be achieved by a conventional buck converter shown in Fig. 13. There are two operating modes, one from time 0 to DT when the switch is on and another from DT to T(1-D) when the switch is off.

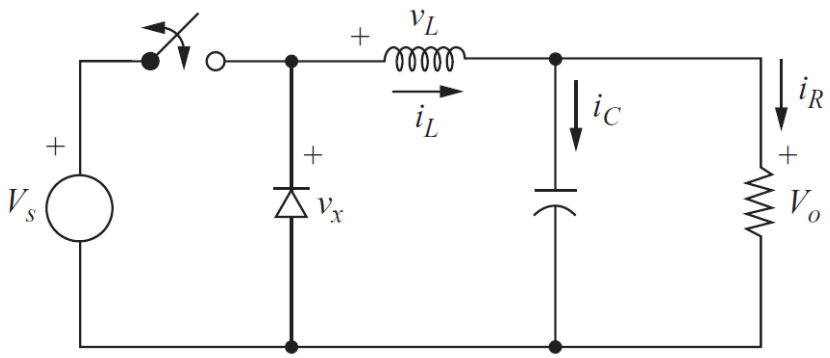

Fig. 13 Buck converter [55]

Operation mode 1 takes place from time 0 to DT. During this period the switch is on and the diode is reverse biased.

$$v_L = V_S - V_o = L\frac{di_L}{dt} \tag{24}$$

This can be arranged as

$$\frac{di_L}{dt} = \frac{V_s - V_o}{L} \tag{25}$$

Since,

$$\frac{di_L}{dt} = \frac{\Delta i_L}{\Delta t} = \frac{\Delta i_L}{DT} \tag{26}$$

Equations (25) and (26) can be combined to find the change in inductor current during T_{on}.

$$(\Delta i_L)_{T_{On}} = \frac{(V_s - V_o)DT}{L} \tag{27}$$

Operation mode 2 takes place from time DT to T(1-D). During this period the switch is off.

$$v_L = -V_o = L\frac{di_L}{dt} \tag{28}$$

This can be arranged as

$$\frac{di_L}{dt} = \frac{-V_o}{L} \tag{29}$$

$$(\Delta i_L)_{T_{Off}} = \frac{-V_o T(1-D)}{L} \tag{30}$$

Net inductor current in steady state operation must be zero over each period T is given as

$$(\Delta i_L)_{T_{On}} + (\Delta i_L)_{T_{Off}} = 0 \tag{31}$$

Substituting equations (27) and (30) into (31) yields equation

$$\frac{(V_s - V_o)DT}{L} + \frac{-V_o T(1-D)}{L} = 0 \tag{32}$$

Simplifying yields

$$G_v = \frac{V_o}{V_s} = D \tag{33}$$

For CCM, the voltage gain is equivalent to D.

4.3.3 Bidirectional DC-DC Buck-Boost Converter

The battery requires the use of a bidirectional DC-DC Buck-Boost converter to charge the batteries. Several topologies for bidirectional Buck-Boost converters are possible, including isolated and non-isolated topologies. The Dual-Active Bridge is one

proposed topology, shown in Fig. 14, useful predominantly for the high power density capability [56]. For specified voltages, this topology allows for the The phase shift allows for control over power flow and voltage gain. Leading phase shift represents forward power flow (battery charging) and lagging phase shifts represent reverse power flow (battery discharging). Controlled soft-switching allows for control over power flow direction. Forward power flow waveforms are shown in Fig. 15.

The average transferred power can be expressed in equation (34).

$$P = \frac{V_i V_o}{n\omega\omega_k}\varphi\left(1 - \frac{\varphi}{\pi}\right) \tag{34}$$

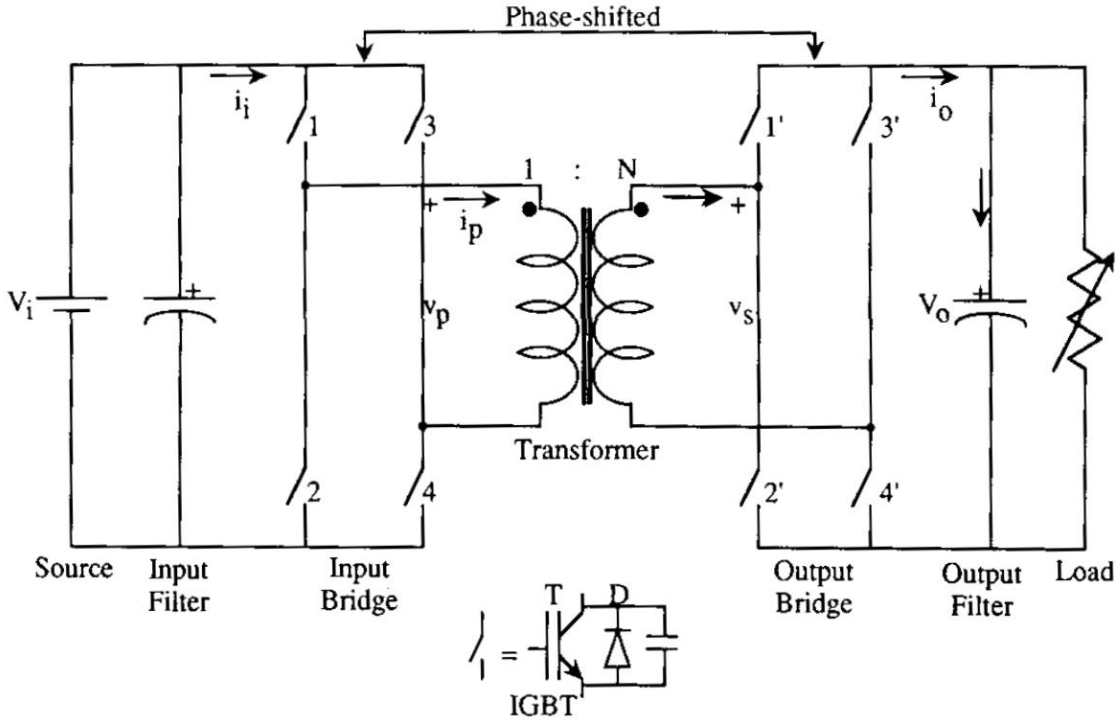

Fig. 14 Dual-Active Bridge bidirectional DC-DC Buck-Boost converter [56]

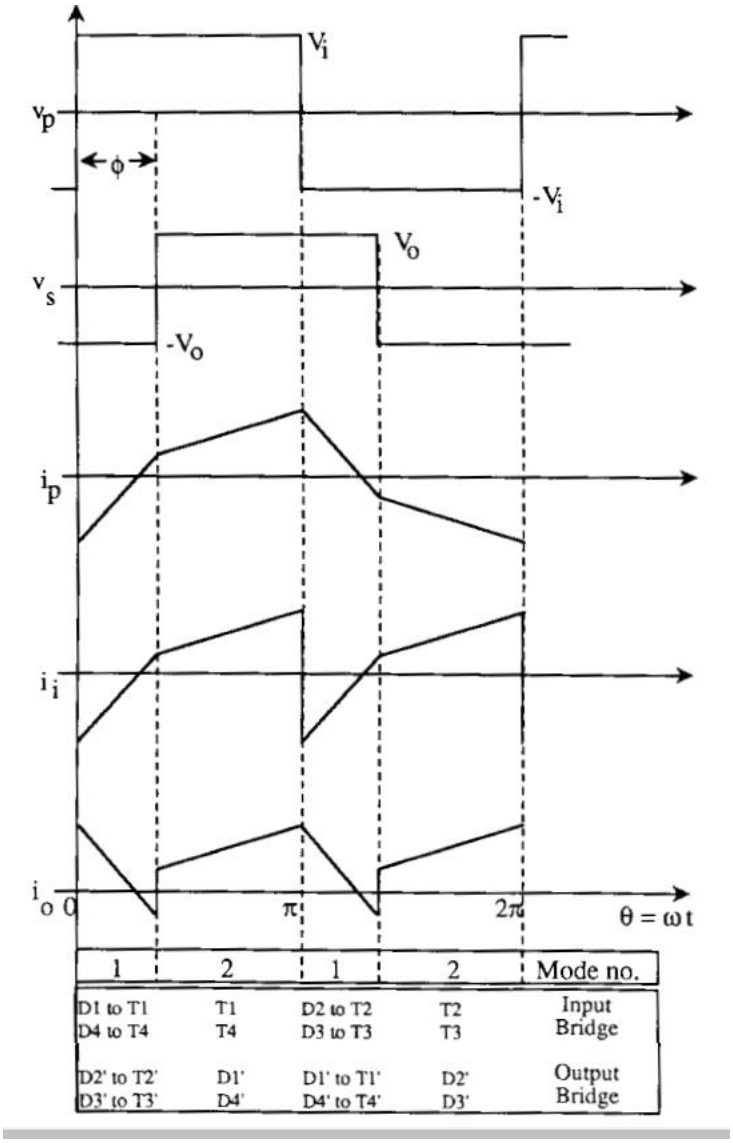

Fig. 15 Idealized operating waveforms of DAB converter [56]

4.3.4 Rectifier

For wind turbine and biomass gasifier generators, a rectifier must be included to convert AC power to DC for connection to the DC bus. While there are some small wind turbines with single phase AC generators, most are three-phase.

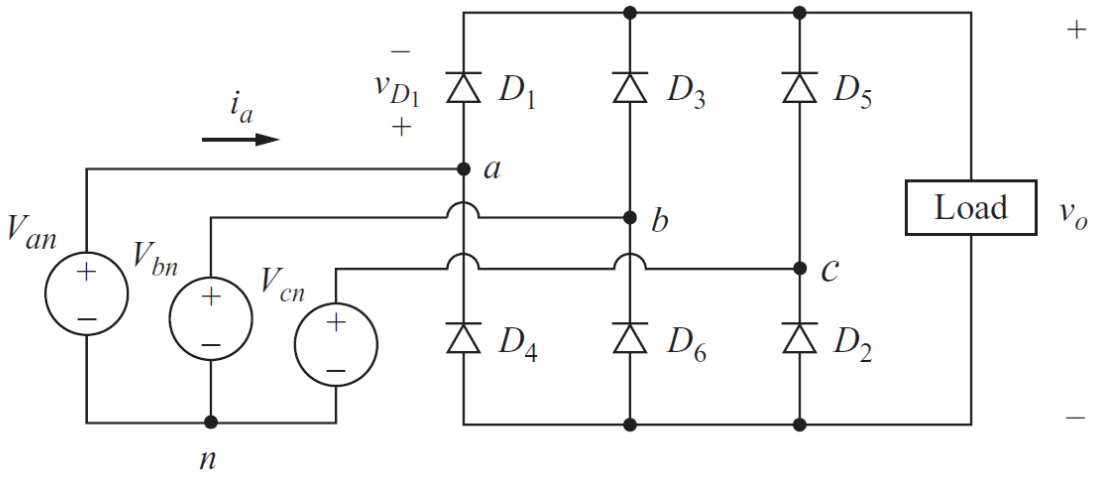

Fig. 16 Three Phase Rectifier [55]

Through carefully timed switching, the three phase rectifier can supply a DC voltage with a ripple to the load. At any given time, Kirchoff's voltage law shows that only a single diode in the top half of the bridge may be in conducting operation, specifically the diode with the anode connected to the highest phase voltage at that instant. Similarly, of the diodes in the bottom half of the bridge, only the diode connected to the lowest voltage phase will conduct at any given instant. The resulting output voltage is equivalent to one of the six line to line voltage of the source. By

replacing the diodes with gate turn-off thyristors, the rectifier can be decoupled from the DC bus in the case of a fault.

4.4 Other Considerations

DC smart meters capable of relaying power usage information to a central system would be a great asset because it would allow technicians to determine where faults might be occurring and it also allows for more detailed information with regards to demand patterns [57]. A DC smart meter could be placed on each home.

On each node, where transmission voltage is stepped down to the utilization voltage, an additional controller can be added to deter and identify theft. The proposed theft deterrence scheme has a constant voltage region and a constant power region of operation, as shown in Fig. 17. Technicians calculate the maximum current and power draw from each node based on the known appliances each home has and inputs these values into the controller. Then the controller sets the duty cycle of the DC-DC converter so that the output voltage is constant equivalent to the reference voltage. A constant power region of control is established when the output current is between the reference current and twice the reference current. When the output current is greater than twice that of the reference current, the duty cycle is turned off. This can deter theft, while still allowing customers to continue to have access to electricity. Technicians will be able to identify which nodes have unauthorized power usage by identifying where the voltage droop is occurring. This is similar to droop control of parallel power generators [42].

$$V_o^* = \begin{cases} V_r & ,I_o \le I_r \\ \frac{P_r}{V_r} & ,2I_r > I_o > I_r \\ 0 & ,I_o > 2I_r \end{cases} \quad (35)$$

where

V_o^*= Controlled output voltage

I_o= Output current

V_r= Reference voltage

I_r= Reference current

P_r=Reference power

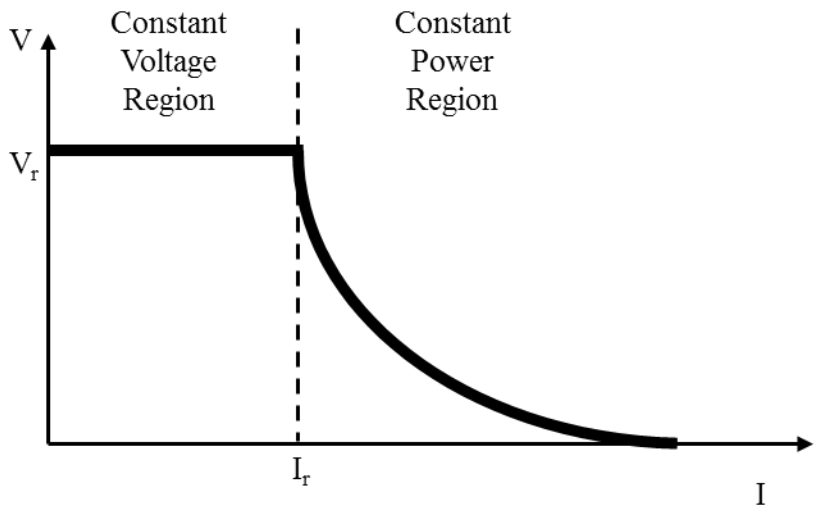

Fig. 17 Proposed theft deterrence scheme I-V characteristic.

5. SIZING METHODOLOGY

Microgrid optimal sizing is necessary to determine the specific topology best suited to the site. This includes selecting the optimal generator type(s) and also determining the number of generating components and amount of energy storage needed. The sizing and topology selection proposed is accomplished by designing each variation possible at a site and then comparing alternatives using financial metrics. Each topological variation is designed using a "worst month" scheme, which can be used in situations where hourly renewable resource data is unavailable. The flowchart in Fig. 18 shows the steps to optimally size the microgrid and select the best topology.

The first step is to collect the local resource data, including both climate and social data, which is used to determine feasibility of generator types. Social data includes monthly income spending and mapping the target population. While hourly wind and solar data is always useful, for many of these locations it is simply not available. As an alternative, the worst monthly average can be used as a design constraint. This thesis will use worst month sizing to generalize the microgrid design applicability to many regions.

Technical constraints are minimum power necessary and generation constraints. For example in a climate with many windless days, a microgrid reliant solely on wind turbines would not be reliable enough, but a hybrid generator topology may still be feasible.

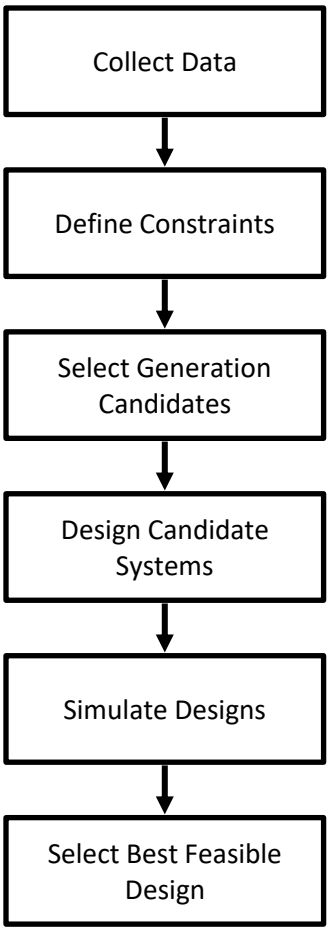

Fig. 18 Sizing methodology

The purchasing power of villagers establishes another constraint. Rural electrification will only succeed in situations where it provides a more inexpensive alternative than traditional energy sources. This means that the monthly cost to consumers must be less than the traditional lighting costs electrical lighting is replacing. If the most inexpensive topology is found to cost more per month than traditional lighting, the microgrid is not financially viable and may require subsidy to operate.

Generation candidates for this paper include wind turbines, PV, and biomass gasifiers, but could be expanded to include wind and micro-hydro as well. In the third

step of the sizing methodology proposed, infeasible generation candidates are eliminated. For example, in a desert region without agriculture a biomass gasifier would not be a feasible generation type to be considered.

After feasible generation types have been selected, each energy ratio is sized by calculating how many generators will be necessary to produce the energy needed daily during the worst month. The best of these alternatives as defined by the lowest cost to end-users for replacing traditional lighting is selected as the optimal topology.

5.1 Power Modeling

For each design variable configuration, power modeling will output the number of each type of generator and energy storage device that is needed. This must be done before financial modeling can be executed.

5.1.1 Demand

One of the benefits of designing rural power systems is that the power consumption is very predictable as the power consumption and variety of appliances each home owns is minimal. Electricity will only be on during service times and even then the load is known explicitly. Both power and energy are two important measurements of demand. The surge demand, or the expected maximum power that may be drawn from the grid, can be calculated with a higher degree of certainty in a mini-grid because the load devices are better known. Daily energy demand can also be calculated more accurately. Power demand can calculated using equation (36).

$$P_p = N_h * P_h + N_{sh} * P_{sh} \tag{36}$$

where

P_p = Peak power demand

N_h = Number of homes

P_h = Power per home

N_{sh} = Number of shops

P_{sh} = Power per shop

The equation used to determine daily energy demand is in equation (37).

$$E_d = P_p * T_s \tag{37}$$

where

E_d = Daily energy demand

T_s = Time of service per day in hours

5.1.2 Solar

Solar irradiance can be measured in solar hours which is measured as the amount of energy per square meter per day and equivalent to the average global daily irradiance. The worst month average number of solar hours per day is used as the resource threshold for solar sizing. To determine the actual power output of the array when used in the field, the rated power must be derated using derating factors. The manufacturing tolerance of the solar cells is included as the manufacturing derating factor. Additionally effects of temperature on the cells are also included as the temperature derating factor. Warmer temperatures reduce cell efficiencies [32]. The temperature derating factor can be calculated using equation (38) and the reference temperature and power temperature coefficient values provided by the manufacturer.

$$f_{temp} = 1 - \gamma(T_{cell} - T_{reference}) \quad (38)$$

where

f_{temp} = Cell temperature derating factor

γ = Power temperature coefficient in % per degree C

Additionally, soil can collect on the arrays. This further reduces the efficiency of the panels and needs to be included as a derating factor. The equation to derate the solar module is given in equation (39).

$$P_{mod} = P_{stc} \times f_{man} \times f_{temp} \times f_{dirt} \quad (39)$$

where

P_{mod} = Derated array power output

P_{stc} = Rated array power output

f_{man} = Manufacturing tolerance derating factor

f_{dirt} = Surface soiling derating factor

The optimal tilt angle can be approximated with equation (40).

$$\beta = 3.7 + 0.69|\varphi| \quad (40)$$

where

β = Optimal tilt angle

φ = Latitude of site

The global horizontal irradiance for a given month can be modified to approximate the global irradiance hitting the surface of the solar panel when tilted at the

optimal tilt angle. The equation to approximate the global irradiance on the tilted plane is given in equation (41).

$$H_{tilt} = \frac{G}{1 - 4.46 \times 10^{-4} \times \beta - 1.19 \times 10^{-4} \times \beta^2} \tag{41}$$

where

G = global horizontal insolence

The number of solar panels needed to satisfy daily demand can be approximated using equation (42). An oversize factor is used to approximate appropriate reliability for the system. Typical oversupply factors for solar are given in table Table 3. The number of solar modules is always rounded up to the nearest integer.

$$N_s = \frac{E_d * f_o}{P_{mod} * H_{tilt} * \eta_{pv}} \tag{42}$$

where

$f_{o,s}$ = Solar panel oversupply factor

η_{pv} = Photovoltaic system efficiency

Table 3 Typical values for oversupply coefficient [58]

Renewable Energy Type	Oversupply Coefficient, f_o
Photovoltaic array	1.3 to 2.0
Micro-hydro generator	1.15 to 1.5
Wind turbine generators	2 to 4

5.1.3 Wind

When considering wind power, first the site's wind power class should be evaluated. In conditions where higher resolution wind resource data is unavailable, the NASA Langley Research Center Atmospheric Science Data Center Surface meteorological and Solar Energy (SSE) web portal contains relevant data sets including monthly average wind speeds over a period of 10 years [59]. Wind power generation relies on consistent and sufficient wind power density, which can be approximated using the wind power classification system. Areas with wind power class 3 resources and above are generally considered suitable for wind energy applications [60], however, in rural areas with lesser power demands areas with wind power class 2 resources may also be suitable. The average wind speed of the worst month should therefore be used to make the assessment of wind power class. If the worst month's average wind power class is greater than class 1, the area is suitable for wind generation. The wind power class can be found in Table 4. To adapt to power densities at different elevations, listed wind speeds should be increased by 3% per 1000m of elevation. The wind profile power law, described by equation (43), allows for wind speeds at various heights to be calculated from a reference height and wind speed. Generally, the power law exponent can be approximated as $1/7^{th}$.

$$\frac{V}{V_r} = \left(\frac{Z}{Z_r}\right)^{\alpha} \tag{43}$$

where

V = Average wind speed at height Z

V_r = Wind speed at reference height, Z_r

Z = Height of average wind speed V

Z_r = Reference height

α = power law exponent

Average power for the worst month can then be found using equation (44). This can be used for sizing by multiplying the average power by 24 hours to find the average energy that can stored per day and determining the minimum number of wind turbines that will satisfy the daily energy demand.

$$P_w = \frac{1}{2}\rho A_w V^3 C_p \tag{44}$$

where

P_w = Average wind turbine power production

ρ = Air density

V = Average month wind velocity

A_w = Swept area of wind turbine rotors

C_p = Power coefficient

The number of wind turbines can be calculated using equation (45). The number of wind turbines should be rounded up to the nearest integer.

$$N_w = \frac{E_d * f_{o,w}}{24 P_w} \tag{45}$$

where

$f_{o,w}$ = Oversupply factor for wind turbines

N_w = number of wind turbines

V = Average month wind velocity

Table 4 Classes of wind power density at 10m and 50m at sea level [60]

Wind Power Class*	**10 m (33 ft)**		**50 m (164 ft)**	
	Wind Power Density (W/m^2)	**Speed(b) m/s (mph)**	**Wind Power Density (W/m^2)**	**Speed(b) m/s (mph)**
1	0	0	0	0
	100	4.4 (9.8)	200	5.6 (12.5)
2				
	150	5.1 (11.5)	300	6.4 (14.3)
3				
	200	5.6 (12.5)	400	7.0 (15.7)
4				
	250	6.0 (13.4)	500	7.5 (16.8)
5				
	300	6.4 (14.3)	600	8.0 (17.9)
6				
	400	7.0 (15.7)	800	8.8 (19.7)
7				
	1000	9.4 (21.1)	2000	11.9 (26.6)

5.1.4 Biomass

Biomass generators are sized using peak power demand and an oversupply factor to determine the rated power size of the biomass gasifier generator. The number of kW that the biomass generator can produce is always rounded up to the nearest integer.

$$P_{bm} = P_d * f_{obm} \tag{46}$$

where

P_{bm} = Battery capacity

P_d = Peak power demand

$f_{o,bm}$ = Oversupply factor for biomass gasifier

5.1.5 Battery Bank

Battery bank energy capacity is calculated using equation (47). Reliability of the system is closely related to the design parameter days of battery bank autonomy for systems with intermittent generators.

$$C_x = \frac{E_{dd}}{V_{dc}} \times \frac{T_{aut}}{DOD_{max}} \tag{47}$$

where

C_x = Battery bank capacity

V_{dc} = Distribution voltage

T_{aut} = Maximum days of autonomy

DOD_{max} = Maximum battery depth of discharge

The number of batteries needed in the battery bank can be calculated using equation (48). The number of batteries should be rounded up.

$$N_{bat} = \frac{C_x}{C_{bat}} \tag{48}$$

where

C_{bat} = Individual battery capacity

5.2 Financial Modeling

Two models are proposed to model financial objectives and constraints. The first uses a levelized cost of electricity calculated using discount rate to calculate the minimum cost of electricity per household. The second uses a nominal cash flow to determine the maximum outflow of cash in a period for the lifetime of a project.

The first model requires the net present cost, presented in equation (49), to be calculated.

$$Net\ Present\ Cost = \sum_{i=s,w,bm,bt} \left(I_i - S_{P_i} + OM_{P_i}\right) \tag{49}$$

where

s = Solar

w = Wind

bm = Biomass

bt = Battery

I_i = Initial cost

S_{P_i} = Present value of salvage value

OM_{P_i} = Present value of operation and maintenance cost for i system equipment

Traditionally, to set a minimum price of electricity for the consumer, the levelized cost of electricity is calculated by dividing the total net present cost over the lifecycle of the project by the total energy produced, shown in equation (37). This LCOE is the minimum price per kWh for utilities to charge their customers in order to breakeven over the lifetime of the project.

$$LCOE = \frac{Total\ Net\ Present\ Cost}{Total\ Energy\ Produced} \tag{50}$$

This establishes the minimum price per unit energy that the utility can charge to breakeven. The margin by which the price is increased is dependent upon competitors pricing and projected demand, among other factors. For the case where the lifetime profit is expected to be zero, so it is assumed that the LCOE is equivalent to the pricing per kWh. Pricing using this method assumes that the revenue over the lifetime of the project must be greater than or equal to the costs over the lifetime of the project, which

can be restated as the profit for the lifecycle of the project must be greater than or equal to zero. The monthly price for basic lighting and cell phone charging can be found by multiplying the monthly energy used for basic lighting and cell phone charging and the LCOE. In the case of a startup, however, two additional constraints are imposed. The first is that deficit spending is not possible due to lack of funds and the second is that pricing must be equal to or less than the amount villagers are able to pay.

The inability for deficit spending requires profits to be greater than or equal to zero throughout the project lifecycle. This can be determined by predicting the outgoing cashflows for every period. There are three cost categories per period: operation and maintenance, replacement of components, and debt repayments.

$$CF_i = OM_i + L_i + R_i \tag{51}$$

where

CF_i = The total cost of period i

OM_i = The total operations and maintenance costs of period i

L_i = The loan payment of period i

R_i = The total replacement costs of period i

The minimum monthly price per household necessary to maintain a profit can be found by finding the maximum average cost to period. The average cost to period determines the average cost of all previous periods up to the current period as described in equation (52).

$$Average\ Cost\ to\ Period = \frac{\sum_{i=1}^{Period} CF_i}{Period} \quad (52)$$

The maximum average cost to period can be converted to cost of electricity by dividing the average cost to period by the amount of energy generated in one period. If the maximum ACTP is larger than the amount that villagers are able to pay, then the topology is an infeasible.

5.2.1 Solar

To calculate the initial cost of solar modules, equation (53) can be used. The cost per solar module should include the raw cost from the distributer of the solar modules and also other costs per solar module such as the supports for each panel. The transmission line conductor will be the same for all alternatives and should not appear in multiple initial cost assessments in hybrid topologies. The lifetime of the solar modules is assumed to longer than the projected lifetime of the project.

$$I_s = \alpha_{sm} * N_s + C_t \quad (53)$$

where

I_s = Initial cost of PV panels

α_{sm} = Cost per solar module

N_s = Number of solar modules

C_t= Cost of transmission line conductor

The salvage value of the solar panels is found using equation (53). The discount rate can be determined by the weighted average cost of capital. In the case of a mini-

utility with a capital structure fully funded by debt, the discount rate is equivalent to the annual interest rate. The inflation rate is the regional inflation rate for the site.

$$S_s = S'_s * N_s * \left(\frac{1+\beta}{1+\gamma}\right)^{T_p} \tag{54}$$

where

S_s = Salvage value of solar panels

S'_s = Salvage value of each solar panel

N_s = Number of solar modules

β = Inflation rate

γ = Discount rate

T_p = Lifetime of project

Operations and maintenance costs can be approximated using equation (55). The escalation rate is used because the operation and maintenance costs escalate at a different rate than the inflation rate. Operations and maintenance assumes that all costs occur at the end of the period.

$$OM_s = (\alpha_{OM_s} * N_s + s_s) * \sum_{i=1}^{T_p} \left(\frac{1+\nu}{1+\gamma}\right)^i \tag{55}$$

where

OM_s = Operation and maintenance for solar panels

α_{OM_s} = Operation and maintenance cost per solar module

N_s = Number of solar modules

ν = Escalation rate

γ = Discount rate

s_s= Salary of one technician

5.2.2 Wind

The initial cost of the wind turbines can be found using equation (56). The lifetime of the wind turbines is assumed to longer than the projected lifetime of the project.

$$I_w = \alpha_w * N_w + C_t \tag{56}$$

where

I_w = Initial cost of wind turbines

α_w = Cost per wind turbine

N_w = Number of wind turbines

The salvage value of the wind turbines can be found using equation (57).

$$S_w = S'_w * N_w * \left(\frac{1+\beta}{1+\gamma}\right)^{T_p} \tag{57}$$

where

S_w = Salvage value of wind turbines

S'_s = Salvage value of each solar panel

N_w = Number of wind turbines

Operations and maintenance costs for the wind turbines can be approximated using equation (58).

$$OM_w = \alpha_{OM_w} * N_w * \sum_{i=1}^{T_p} \left(\frac{1+\nu}{1+\gamma}\right)^i \quad (58)$$

where

OM_w = Operation and maintenance for wind turbines

α_{OM_w} = Operation and maintenance cost per wind turbine

N_w = Number of wind turbines

5.2.3 Biomass

The initial cost of a biomass gasifier is approximated using equation (59).

$$I_{bm} = \alpha_{bm} * P_{bm} \quad (59)$$

where

I_{bm} = Initial cost of biomass gasifier

α_{bm} = Cost per kW for biomass generator

P_{bm} = Rated power of biomass gasifier

The salvage value of the biomass gasifier is given in equation (60).

$$S_{bm} = S'_{bm} * P_{bm} * \left(\frac{1+\beta}{1+\gamma}\right)^{T_p} \quad (60)$$

where

S_{bm} = Salvage value of biomass gasifier

S'_{bm} = Salvage value of each biomass gasifier

P_{bm} = Rated power of biomass gasifier

Operation and maintenance for the biomass generator is given in equation (61). The biomass gasifier will require partial replacement every 11,000 operating hours and is assumed to need to be replaced more frequently than the lifetime of the project. Additionally, unlike wind and solar energy, the biomass gasifier will require four technicians during operation to feed the biomass into the gasifier.

$$OM_{bm} = \left(\alpha_{OM_{bm}} * P_{bm} + k_f + s\right) * \sum_{i=1}^{T_p} \left(\frac{1+\nu}{1+\gamma}\right)^i + OM_{bm,r} \tag{61}$$

where

OM_{bm} = Operation and maintenance for biomass gasifier

$\alpha_{OM_{bm}}$ = Operation and maintenance cost per kW

P_{bm} = Rated power of biomass gasifier

k_f = Cost of fuel

s = Salary of technicians

$OM_{bm,r}$ = Replacement costs

Fuel costs are calculated using the energy of rice per kg. Using the lowest energy density of rice, rice husks are estimated to contain 12.6 MJ per kg [61, 62]. The efficiency of the biomass gasifier can be estimated to be 20% [62].

$$k_f = \frac{E_d}{E_r * \eta_{bm}} * \frac{365}{1000} * c_{rh} \tag{62}$$

The replacement cost can be represented by equation (63).

$$OM_{bm,r} = \alpha_{bm,r} * P_{bm} * \sum_{i=2}^{X_{bm}} \left(\frac{1+\nu}{1+\gamma}\right)^{(i-1)T_{bm}} \tag{63}$$

where

OM_{bm} = Operation and maintenance for biomass gasifier

$\alpha_{bm,r}$ = Biomass replacement cost per kW

X_{bm} = Number of biomass gasifier replacements needed over lifetime of the project

T_{bm} = Lifecycle of biomass gasifier

5.2.4 Battery Bank

The capital cost for the battery bank is calculated by equation (64).

$$I_{bat} = \alpha_{bat} * N_{bat} \tag{64}$$

where

I_{bat} = Initial cost of batteries

α_{bat} = Cost per battery

N_{bat} = Number of batteries

X_{bat} = Number of times batteries must be purchased during the project life span

T_{bat} = Battery lifespan

Operations and maintenance costs are approximated in equation (65).This includes battery replacement costs.

$$OM_{bat} = \alpha_{OM_{bat}} * N_{bat} * \sum_{i=1}^{T_p} \left(\frac{1+\nu}{1+\gamma}\right)^{i} + OM_{bat,r} \tag{65}$$

where

OM_{bat} = Operation and maintenance for batteries

$\alpha_{OM_{bat}}$ = Operating and maintenance cost per battery

N_{bat} = Number of batteries

$OM_{bat,r}$ = Replacement costs

The replacement cost can be represented by equation (66).

$$OM_{bat,r} = \alpha_{bat,r} * P_{bat} * \sum_{i=2}^{X_{bat}} \left(\frac{1+\nu}{1+\gamma}\right)^{(i-1)T_{bat}} \quad (66)$$

where

OM_{bat} = Operation and maintenance for battery bank

$\alpha_{bat,r}$ = Battery replacement cost per battery

X_{bat} = Number of battery bank replacements needed over lifetime of the project

T_{bat} = Lifecycle of battery bank

5.3 Hybrid Modeling and Optimization

Hybridization of generator technologies in many circumstances can be more cost efficient and reliable than a microgrid dependent on a single generator type. To determine the best mixture of multiple generation sources, an optimization or enumeration method must be applied. The proposed design variables are the amount of daily energy provided by each generation type candidate. The proposed method of this thesis is to use the worst month sizing scheme to size the generators and then calculate the minimum monthly cost to the consumer for basic lighting during the service hours. This process is then done incrementally until the design space has been sufficiently explored and then the minimum objective value can be used to indicate what topology is optimal.

In the case that there are two generator types being considered, the value F can represent the ratio of one of the generator types. Intervals of *F* values need to be small enough to fully explore the design space. Additionally the design space of the hybrid includes single generator topologies. In the case where two generator types are being considered, the *F* values at 0 and 1 represent single generator topologies.

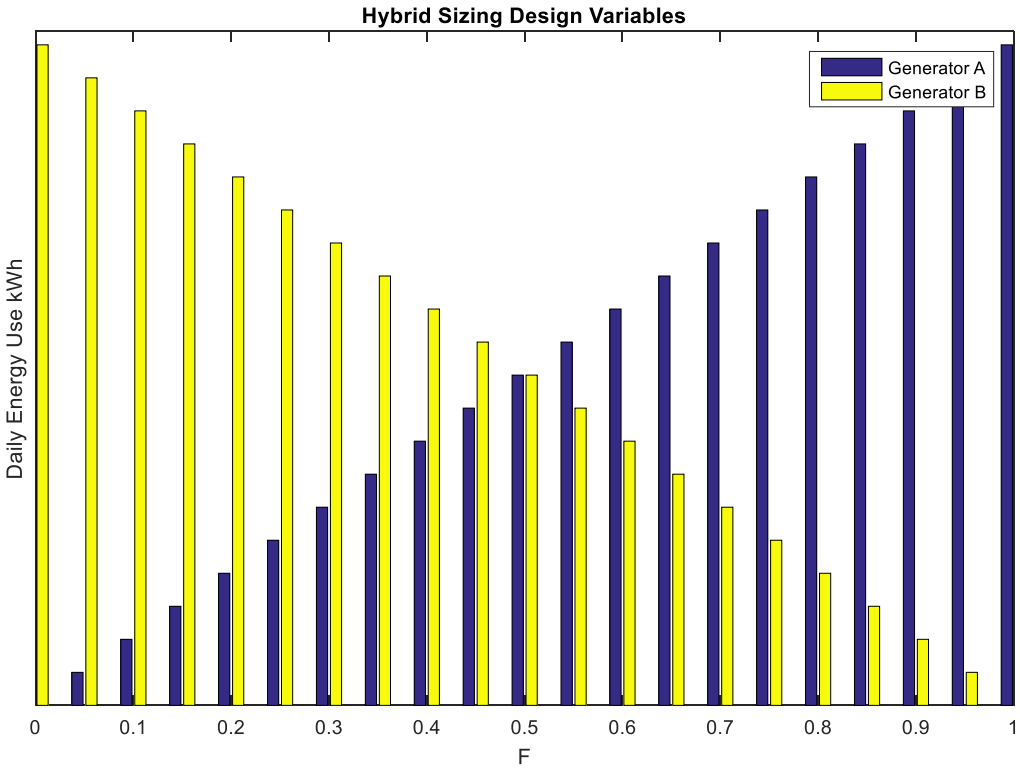

Fig. 19 Design variables used for hybrid sizing optimization.

6. CASE STUDY

6.1 Model Village

To better illustrate this methodology a case study featuring a model of a typical village is presented. The state of Bihar has one of the lowest electrification rates in India [63]. Bihar is also in a region known as the “rice belt” of India, which produces a majority of the rice in the country. The model village has 450 households and 20 shops. All 450 households are within a 1 mile radius of the village center. Households purchase kerosene for lighting at night and spend approximately $2.50 per month on kerosene for lighting and also to charge their cellphones in the nearest village. The village is a candidate for electrification to replace kerosene for lighting. Each home will receive 3 LED lights and will have a peak power consumption of 30 Watts. Each shop will receive 6 LED lights and have a peak power consumption of 60 Watts.

Table 5 Case Study model village information

Number of Households	450
Number of Shops	20
Household Power	30 Watts
Shop Power Demand	60 Watts
Monthly Traditional Energy Spending	$2.50
Total Initial Service Hours Needed	6 Hours

The capital required for the project will be financed from a soft loan with monthly payments over a period of 5 years at an annual interest rate of 5% with monthly compounding periods.

Table 6 Case study loan information

Payment period	Monthly
Compounding Period	Monthly
Nominal Annual Interest Rate	5%
Loan term	5 years

6.2 Local Resources

For this model village, it was assumed that the only data available is from the Solar and Wind Energy Resource Assessment (SWERA) tool from NREL, which provides monthly averages based on NASA GIS datasets. Table 7 shows that the minimum average daily horizontal insolation is 3.46 kWh/m^2/day, which is sufficient for it to be considered as a generation candidate because it is greater than the 3 kWh/m^2/day threshold.

Wind resources for the region, however, are wind power class 1 for all months and are therefore not considered as a solution. Therefore, wind will not be considered as a generation candidate.

Rice husks are common in Bihar and contain large amounts of silica, which prevents them from being used as fertilizer or livestock feed. Rice husks are left to rot, which emitting CO2 during the decomposition process, or is burnt [62]. The minimum amount of energy in a kg of rice husks is about 12.6 MJ [61]. Bihar produces an

estimated 1.8 billion kg of rice husks a year, with rice production increasing annually [63, 64]. Prices for rice husks locally are around $25 per metric ton [62].

Therefore solar and biomass generators are feasible for consideration, but wind turbines are not.

Table 7 Local resource data for model village [59]

Month	Average daily Global insolation (kWh/m^2/day	Average wind speed (m/s)
January	3.46	2.26
February	4.87	2.72
March	6.23	2.73
April	6.83	3.42
May	6.82	3.8
June	5.82	3.75
July	4.96	3.17
August	5.25	2.73
September	5.01	2.55
October	4.94	2.04
November	4.35	2.02
December	3.48	2.12

6.3 Design Parameters

6.3.1 Solar

Discrete number of solar panels and batteries could be purchased with this methodology. The PV modules modeled were based on the Jinhua Dokio Technology DSP80-290P modules, polycrystalline type cells rated at 80 Wp with a 25 year [65]. The manufacturing tolerance was given as 2%, therefore the correlating estimated

manufacturing derating factor for the solar panels is 98%. The soiling derating factor for the solar panels was estimated at 97%.

6.3.2 Battery Bank

The total cost of each battery in the battery bank costs $110 and has a capacity of 35 Ah.

6.3.3 Biomass

A discrete number amount of power could be provided by a biomass gasifier. For example, a biomass gasifier could be rated for 8 kW but not 8.2 kW. This is to reflect the difficulty in manufacturing or purchasing a gasifier when the rated power is too specific.

6.3.4 Hybrid

The hybridization combined the solar, battery, and biomass generator power sizing and financial modeling.

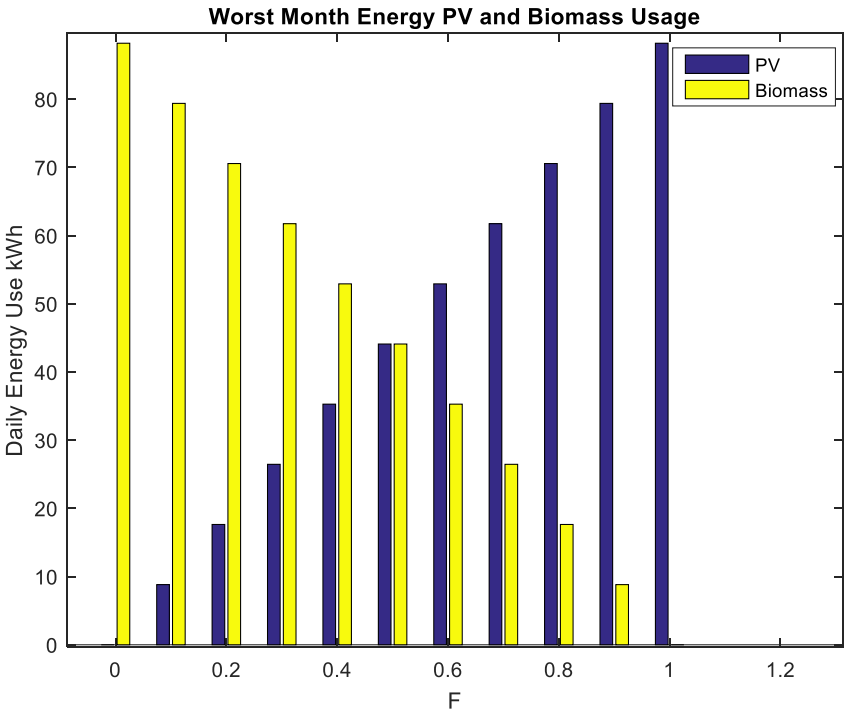

Fig. 20 Hybrid F-value energy usage plot

Table 8 Case study design parameters

Description	**Symbol**	**Value**
Solar panel cost		$0.45/W [65]
Total cost per solar panel	α_s	$0.70/module
Solar panel surface size		1000 mm x 862 mm [65]
Solar panel rated power	P_{stc}	80 W [65]
Solar panel derated power	P_{mod}	73.4 W
Solar panel lifetime		25 Years [65]
Solar panel power temperature coefficient	γ	0.005 % per ° C [65]
Average solar cell temperature		32° C [59]
Solar cell temperature derating factor	f_{temp}	96.5%
Solar panel manufacturing derating factor	f_{man}	98%
Solar panel surface soiling derating factor	f_{soil}	97%
Solar panel oversupply factor	$f_{o,s}$	1 to 2
Battery cost	α_{bat}	$110/Battery
Battery capacity	C_{bat}	35 Ah
Battery lifetime	T_{bat}	10 years
Depth of discharge	$DOD_{\max}$	50%
Biomass lifetime	T_{bm}	11,000 operating hours [66]
Biomass generator cost	α_{bm}	$1500/kW [62]
Biomass fuel price	k_f	$30/tonne [62]

6.4 Results and Discussion

By minimizing the maximum average cost to period, the optimal microgrid architecture was found to be a hybrid architecture with 396 solar panels, 20 batteries, and a 6 kW biomass gasifier generator, which required a minimum monthly payment of $2.35 for basic electricity usage. The loan payment the optimal size was $654.23. The solar panels were arranged in 66 parallel strings of 6 panels each. The batteries are arranged in a single string of 20 batteries in series.

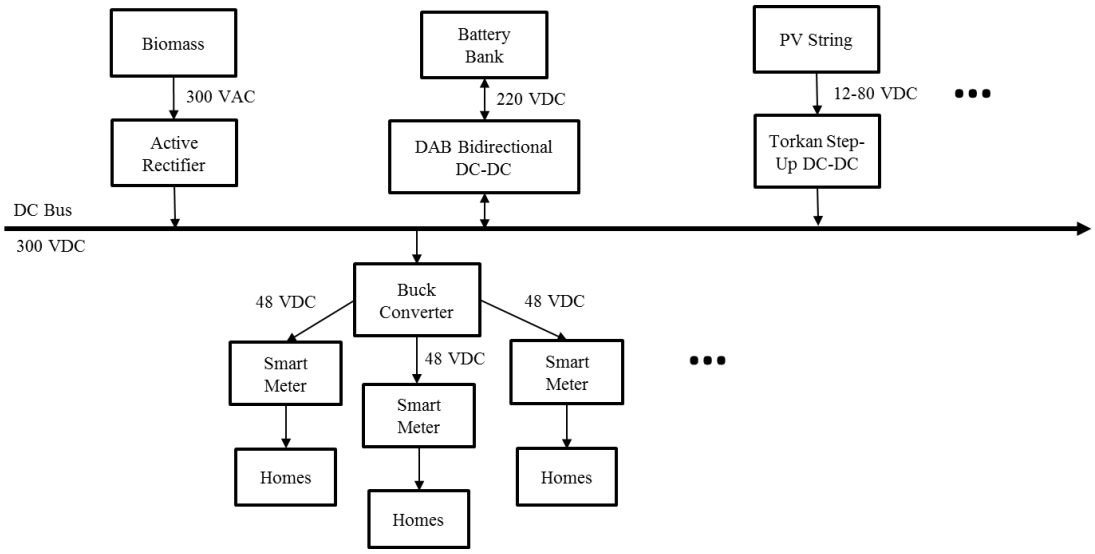

Fig. 21 Proposed architecture of microgrid solution

The nominal cash flows of the three microgrid architectures are presented in Fig. 22, Fig. 23, and Fig. 24. The cash flow is composed of operation and maintenance, loan payments, and periodic battery and biomass generator replacements. The battery bank requires full replacement every 10 years. The biomass generator requires partial replacement every 5 years. The maximum average cost to period can be calculated from these nominal cash flows. A major benefit solar has over biomass is that the replacement costs occur after the loan has reached maturity, allowing the maximum average cost to period of the architectures relying on a majority of daily energy demand to be provided by solar to not include a loan payment. In general, the cash flow profile of solar tends to be lower operational costs, but larger upfront cost, whereas the cash flow profile of biomass tends to have a steady cost that increases due to inflation. The maximum of the solar average cost to period occurs at the end of year 5 and the maximum of the biomass average cost to period occurs at the end of year 20. The optimal microgrid architecture

maximum average cost to period balances the high costs of solar in the first 5 years and the high cost of biomass in the future.

Significantly, were the LCOE used as the objective instead as is the current standard, a completely different architecture would have been chosen that would have quickly encountered cash flow issues. An architecture chosen from its LCOE would have run into cash flow deficits soon after launching. Even in the circumstances where the cash flow deficit was caught, the pricing of energy necessary to eliminate the cash flow issues would be greater than the $2.50 threshold established earlier, effectively creating a significant economic barrier to accessing electricity within the community, which would further contribute to the failure of the business.

Table 9 Optimal microgrid size and corresponding metrics

Description	**Value**
F	.627
Number of solar panels	396
Number of batteries	20
Rated power of biomass gasifier	6 kW
MACP COE	$0.45/kWh
NPC	$249,846

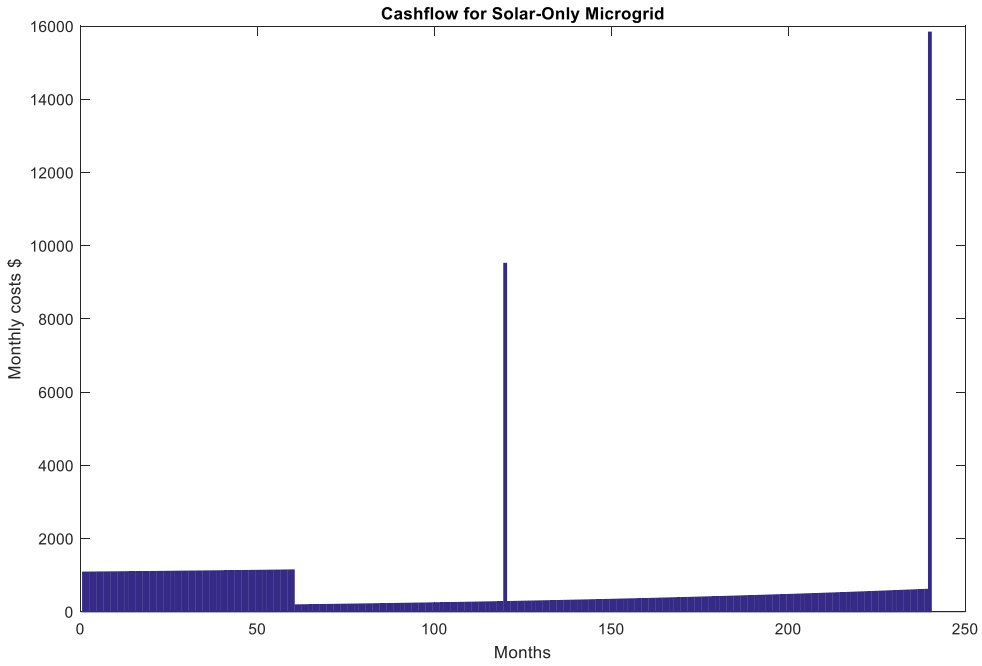

Fig. 22 Projected nominal cash flow for Solar-only topology

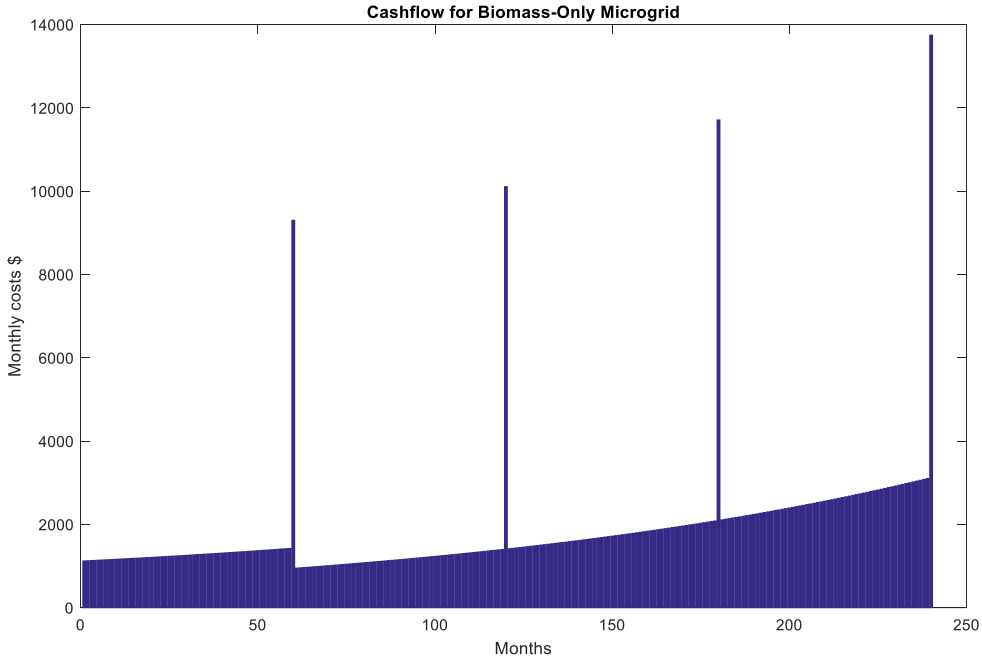

Fig. 23 Projected nominal cash flow for Biomass-only topology

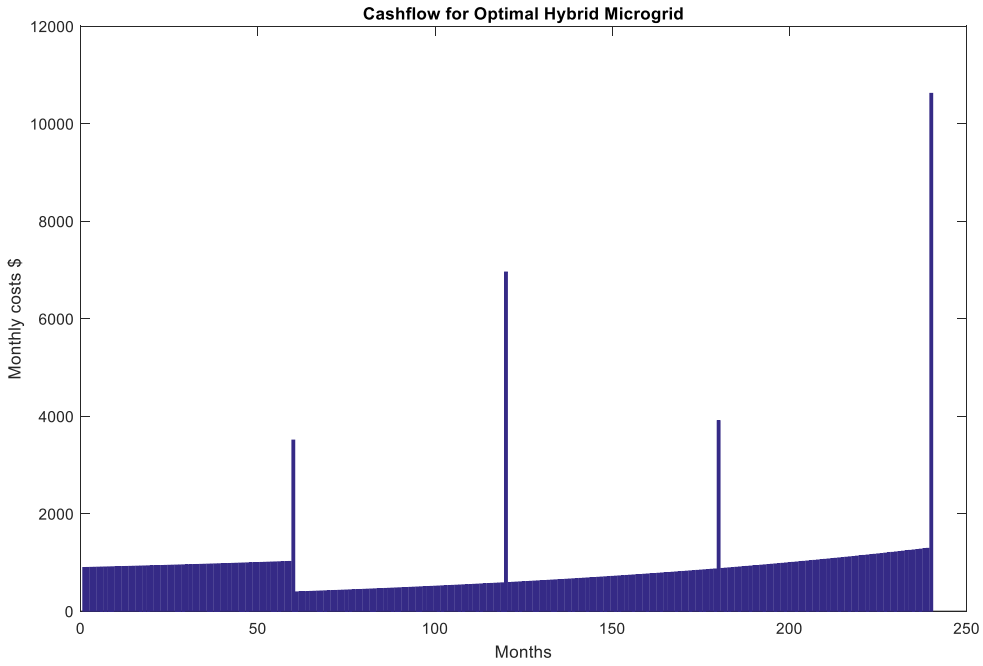

Fig. 24 Projected nominal cash flow for optimal hybrid topology

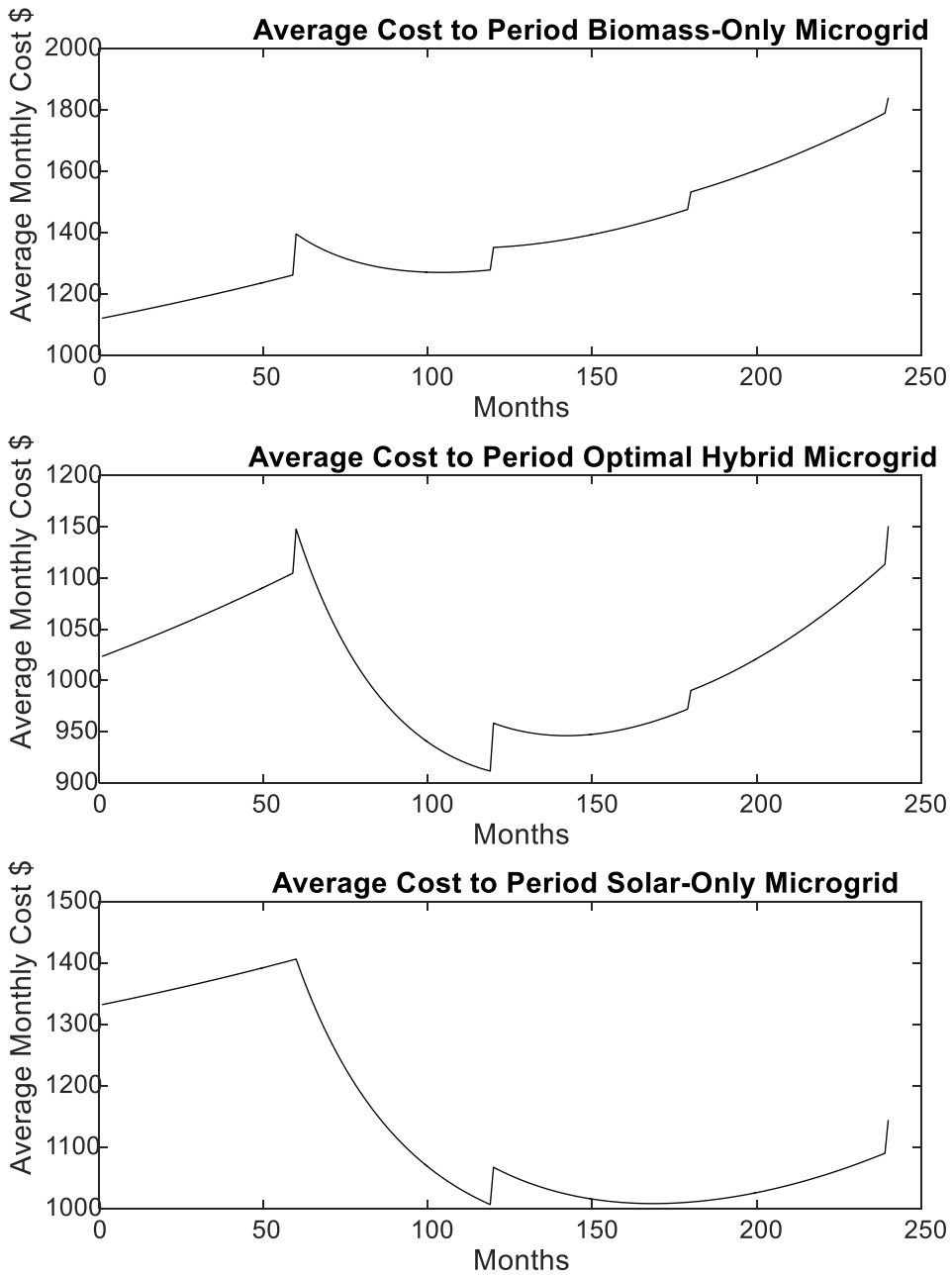

Fig. 25 Average cost to period of various microgrid architectures

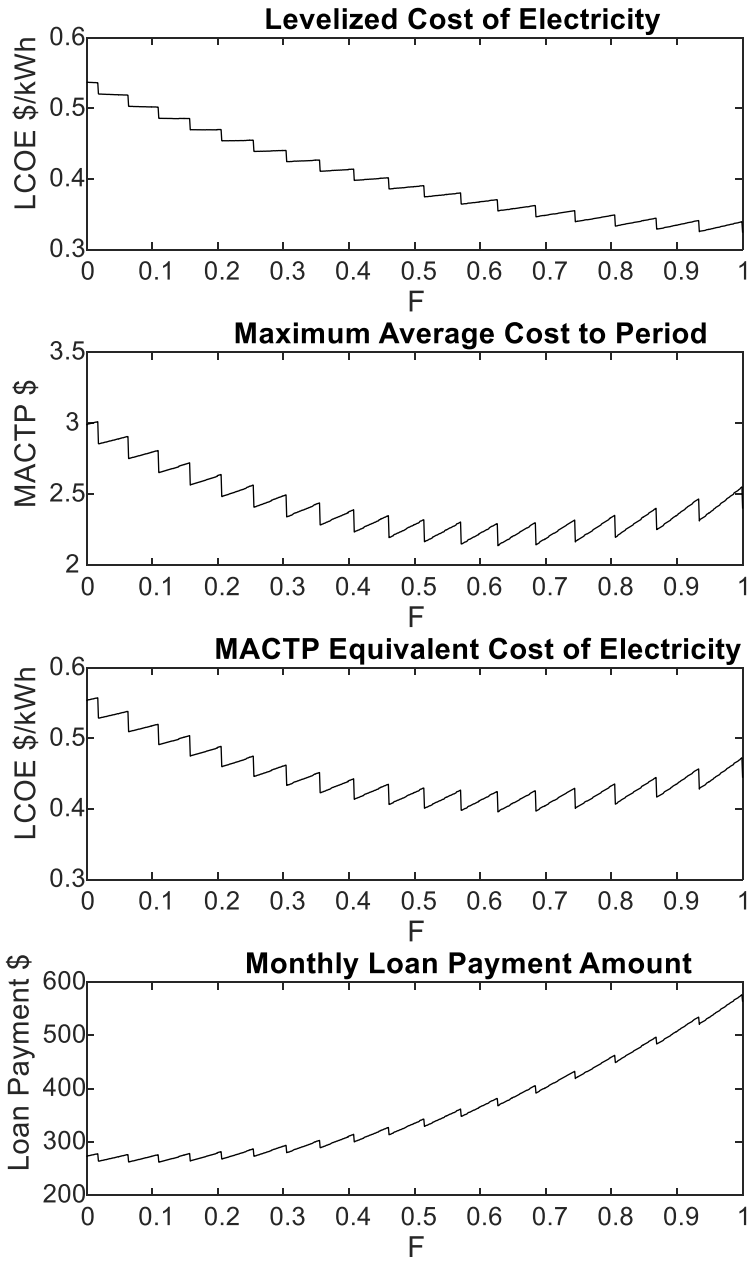

Fig. 26 Plots of hybrid sizing economic metrics with 5 year loan at 5% interest

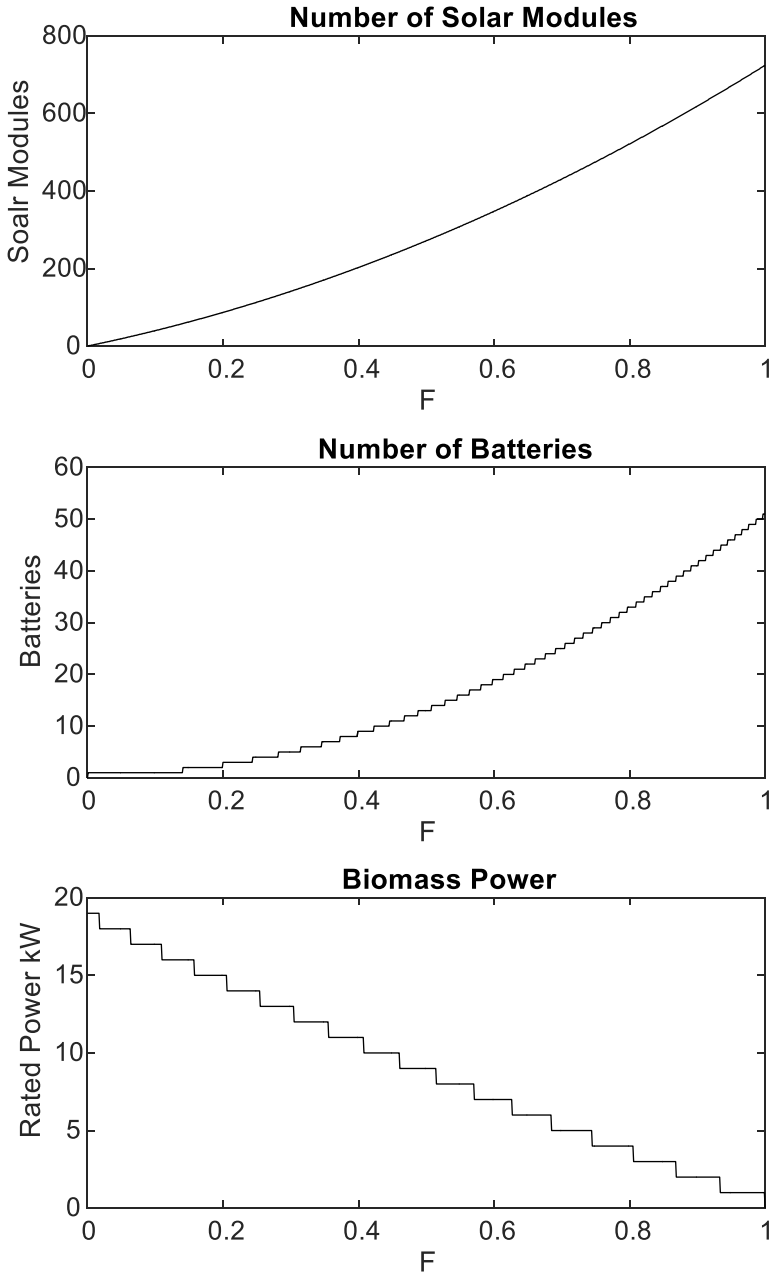

Fig. 27 Sizes of solar modules, batteries, and biomass generators for hybrid system

Table 10 Topology metric comparison

Generator	NPC	LCOE	Monthly Payment based on LCOE	MACTP COE	MACTP
Solar	$208,551	0.32 $/kWh	$1.75	0.53 $/kWh	$2.87
Biomass	$397,272	0.62 $/kWh	$3.33	0.70 $/kWh	$3.75
Hybrid	$244,759	0.38 $/kWh	$2.05	0.44 $/kWh	$2.35

6.5 Effect of Loan Period

The loan period was also found to make a considerable difference in determining the optimal architecture and sizing. The effect of the loan period is shown in Table 11. Longer loan periods were found to correspond to lower monthly end-user payment and an increasing preference for solar panels over biomass generation. This of course comes at the cost of local entrepreneurs who will only achieve full ownership when the loan is paid off. Longer loan periods also correlates with larger risk on the part of the loaning institution and loan rates may be higher to match the increased risk on the behalf of the loaning institution. Shorter loan periods penalize higher capital cost, whereas longer loan periods impose a lesser penalty on capital cost. The longer the loan period, the more capital intensive architectures with low operation and maintenance costs are preferred. Therefore, under conditions where long term loans are possible, solar and wind technologies are more likely to be optimal.

Table 11 Effect of loan period on optimal topology and monthly customer payment

Loan Period	Alternative with Lowest Monthly Payment	Monthly End-user Payment for Lighting
5	Hybrid	$2.35
7.5	Hybrid	$2.27
10	Hybrid	$2.23
12.5	Hybrid	$2.16
15	Solar	$2.11

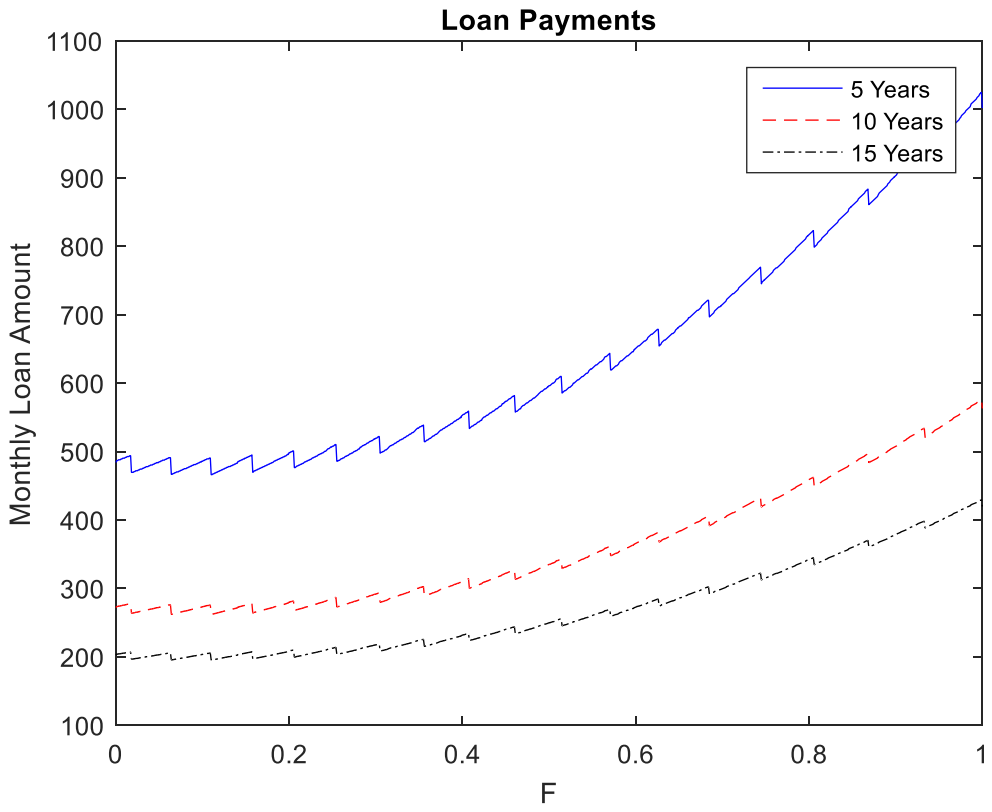

Fig. 28 Monthly loan payment amount for various loan periods

7. CONCLUSIONS AND FUTURE WORK

7.1 Conclusions

This work describes a socio-economically sustainable mini-utility planning approach for rural electrification in developing countries. A DC microgrid architecture was chosen because most end-uses for electricity in the developing world are natively DC. Additionally, DC microgrid architecture is most appropriate for PV, which outputs DC power, as well as small wind turbines, which are more efficient in DC systems than AC systems. Overall, the microgrid architecture focused on simple operation, capable of being operated by local technicians rather than engineers. A methodology was presented for site-specific microgrid sizing in situations where minimal wind and solar resource data is available. Metrics used to compare alternatives included net present project as well as consumer-side metrics such as LCOE and minimum monthly payments per household necessary to breakeven. Minimization of cost to consumers was outlined and the holistic design of this work was generalized for usage in variety of geographic, societal, economic, and political environments.

A case study was presented in which a microgrid was sized for a model village in the state of Bihar, India under conditions where high temporal resolution resource data was not available. The results of the case study showed the deficiencies of minimizing levelized cost of electricity or net present cost as an optimization objective when taking loan periods less than the life of the project into account. As an alternative to using the financial metric net present value when evaluating rural electrification projects, maximum average cost to period calculated using nominal cash flow analysis was

proposed. Maximum average cost to period includes the constraint that mini-utilities are not financially viable if they require a deficit during any period, which is not acknowledged in the net present cost approach. Optimization of microgrid architecture utilizing maximum average cost to period can also provide a realistic estimate of the actual monthly cost to end-users which is essential due to the low purchasing power of end-users. Additionally, the case study also showed the loan period has a significant effect on the optimal microgrid architecture as shorter loan periods impose more severe economic penalties on capital intensive technologies such as solar panels and wind turbines.

7.2 Future Work

Rural electrification is constantly developing and recently has found renewed attention from the global community. Due to the great importance in improving rural electrification access, much of this work will continue to be developed. Additional generation technologies such as small or micro hydro will be added as potential generation types to fully utilize local sources. Reliability simulations of loss of load will also be added. Wind speed simulations utilizing Weibull distributions will be further researched. Other methods of DC grounding will also be explored such as monopolar earth grounding. Growth of community power demand over time is also of significant interest to this research.

REFERENCES

[1] *Sustainable Energy for All 2015 - Progress Toward Sustainable Energy,* The World Bank and the International Energy Agency, Washington D.C., 2015.

[2] "World Energy Outlook 2016 - Electricity Access Database," International Energy Agency, 2016.

[3] A. Zomers, “Remote Access: Context, Challenges, and Obstacles in Rural Electrification,” *IEEE Power and Energy Magazine,* vol. 12, no. 4, pp. 26-34, 2014.

[4] S. Ray, B. Ghosh, S. Bardhan, and B. Bhattacharyya, “Studies on the impact of energy quality on human development index,” *Renewable Energy,* vol. 92, pp. 117-126, 2016.

[5] N. S. Ouedraogo, “Energy consumption and human development: Evidence from a panel cointegration and error correction model,” *Energy,* vol. 63, pp. 28-41, 2013.

[6] L. Grogan, and A. Sadanand, “Rural Electrification and Employment in Poor Countries: Evidence from Nicaragua,” *World Development,* vol. 43, pp. 252-265, 2013.

[7] A. Jhunjhunwala, “The people's grid,” *IEEE Spectrum,* vol. 54, no. 2, pp. 44-50, February 207, 2017.

[8] T. Slough, J. Urpelainen, and J. Yang, “Light for all? Evaluating Brazil's rural electrification progress, 2000–2010,” *Energy Policy,* vol. 86, pp. 315-327, 2015.

[9] B. Mainali, S. Pachauri, N. D. Rao, and S. Silveira, “Assessing rural energy sustainability in developing countries,” *Energy for Sustainable Development,* vol. 19, pp. 15-28, 2014.

[10] *Key World Energy Statistics 2016*, International Energy Agency, Paris, France, 2016.

[11] *BP Statistical Review of World Energy 2016*, BP, London, UK, 2016.

[12] N. L. Lam, K. R. Smith, A. Gauthier, and M. N. Bates, “Kerosene: a review of household uses and their hazards in low- and middle-income countries,” *Journal of Toxicology and Environmental Health, Part B,* vol. 15, no. 6, pp. 396-432, 2012.

[13] N. L. Lam, Y. Chen, C. Weyant, C. Venkataraman, P. Sadavarte, M. A. Johnson, K. R. Smith, B. T. Brem, J. Arineitwe, J. E. Ellis, and T. C. Bond, “Household light makes global heat: high black carbon emissions from kerosene wick lamps,” *Environmental Science and Technology,* vol. 46, no. 24, pp. 13531-8, Dec 18, 2012.

[14] M. Ehsani, and H. M. K. Al-Masri, "Engineering and socio-economic aspects of sustainable energy." pp. 368-371.

[15] R. A. Muller, *Energy for Future Presidents: The Science Behind the Headlines*: W. W. Norton & Company, 2012.

[16] B. Mainali, and S. Silveira, “Using a sustainability index to assess energy technologies for rural electrification,” *Renewable and Sustainable Energy Reviews,* vol. 41, pp. 1351-1365, 2015.

[17] E. Ilskog, “Indicators for assessment of rural electrification—An approach for the comparison of apples and pears,” *Energy Policy,* vol. 36, no. 7, pp. 2665-2673, 2008.

[18] M. Ranaboldo, B. Domenech, G. A. Reyes, L. Ferrer-Martí, R. Pastor Moreno, and A. García-Villoria, “Off-grid community electrification projects based on wind and solar energies: A case study in Nicaragua,” *Solar Energy,* vol. 117, pp. 268-281, 2015.

[19] Y. Sawle, and S. C. Gupta, "Optimal sizing of photo voltaic/wind hybrid energy system for rural electrification." pp. 1-4.

[20] A. Garba, and M. Kishk, "A techno-economic comparison of biomass thermo-chemical systems for sustainable electricity in Nigerian rural areas." pp. 1-6.

[21] S. H. Alalwani, "Optimal techno-economic unit sizing of hybrid PV/Wind/battery energy system for an islanded microgrid using the forever power method." pp. 1-8.

[22] M. S. Abdulah, T. Matlokotsi, and S. Chowdhury, "Techno-economic feasibility study of solar PV and biomass-based electricity generation for rural household and farm in Botswana." pp. 67-71.

[23] M. Kolhe, K. M. I. Ranaweera, and A. G. B. S. Gunawardana, "Techno-economic analysis of off-grid hybrid renewable energy system for Sri Lanka." pp. 1-5.

[24] A. Gupta, R. P. Saini, and M. P. Sharma, "Steady-state modelling of Hybrid Energy System." pp. 1-10.

[25] S. Kumaravel, S. Ashok, and P. Balamurugan, "Techno-economic feasibility study of biomass based hybrid renewable energy system for microgrid application." pp. 107-110.

[26] *From Gap to Opportunity : Business Models for Scaling Up Energy Access*, International Finance Corporation, Washington, DC, United States, 2012.

[27] *Cell Phones in Africa: Communication Lifeline*, Pew Research Center, 2015.

[28] H. Zerriffi, *Rural electrification: strategies for distributed generation*: Springer Science & Business Media, 2010.

[29] X. Zhang, and A. Kumar, "Evaluating renewable energy-based rural electrification program in western China: Emerging problems and possible scenarios," *Renewable and Sustainable Energy Reviews,* vol. 15, no. 1, pp. 773-779, 2011.

[30] J. Goldemberg, E. L. La Rovere, and S. T. Coelho, "Expanding access to electricity in Brazil," *Energy for sustainable development,* vol. 8, no. 4, pp. 86-94, 2004.

[31] D. Neves, C. A. Silva, and S. Connors, "Design and implementation of hybrid renewable energy systems on micro-communities: A review on case studies," *Renewable and Sustainable Energy Reviews,* vol. 31, pp. 935-946, 2014.

[32] A. Luque, and S. Hegedus, *Handbook of Photovoltaic Science and Engineering*, Second ed., Chichester, West Sussex, U.K: Wiley, 2011.

[33] D. Feldman, R. Margolis, A. Goodrich, G. Barbose, R. Wiser, and N. Darghouth, *Photovoltaic (PV) Pricing Trends: Historical, Recent, and Near-Term Projections*, NREL, 2012.

[34] A. Tummala, R. K. Velamati, D. K. Sinha, V. Indraja, and V. H. Krishna, "A review on small scale wind turbines," *Renewable and Sustainable Energy Reviews*, vol. 56, pp. 1351-1371, 2016.

[35] A. A. L. Zaharia, S. Brisset, and M. M. Radulescu, "Modeling approaches to brushless DC permanent-magnet generator for use in micro-wind turbine applications." pp. 445-451.

[36] O. C. Onar, Y. Gurkaynak, and A. Khaligh, "A brushless DC generator & synchronous rectifier for isolated telecommunication stations." pp. 1-6.

[37] J. Kwon, X. Wang, C. L. Bak, and F. Blaabjerg, "Analysis of harmonic coupling and stability in back-to-back converter systems for wind turbines using Harmonic State Space (HSS)." pp. 730-737.

[38] J.-P. Badeau, and A. Levi, *Renewable Energy: Research, Development and Policies : Biomass Gasification : Chemistry, Processes and Applications*, New York, US: Nova, 2009.

[39] A. Lantero. "The War of the Currents: AC vs. DC Power," https://www.energy.gov/articles/war-currents-ac-vs-dc-power.

[40] Y. Wang, Z. Yu, J. He, S. Chen, R. Zeng, and B. Zhang, "Performance of Shipboard Medium-Voltage DC System of Various Grounding Modes Under

Monopole Ground Fault," *IEEE Transactions on Industry Applications,* vol. 51, no. 6, pp. 5002-5009, 2015.

[41] *HVDC Classic Transmission References*, Siemens, Erlangen, Germany, 2012.

[42] M. Shadmand, "MODEL PREDICTIVE CONTROL TECHNIQUES WITH APPLICATION TO PHOTOVOLTAIC, DC MICROGRID, AND A MULTI-SOURCED HYBRID ENERGY SYSTEM," Dissertation, Electrical and Computer Engineering Department, Texas A&M University, 2015.

[43] R. E. Nabours, "Dalziel revisited," *IEEE Industry Applications Magazine,* vol. 15, no. 3, pp. 18-21, 2009.

[44] A. Sandeep, and B. G. Fernandes, "Optimal Voltage Level for DC Microgrids," in IECON 2010 - 36th Annual Conference on IEEE Industrial Electronics Society, Glendale, AZ, 2010, pp. 3034-3039.

[45] L. Weixing, M. Xiaoming, Z. Yuebin, and C. Marnay, "On voltage standards for DC home microgrids energized by distributed sources." pp. 2282-2286.

[46] N. L. Lam, S. Pachauri, P. Purohit, Y. Nagai, M. N. Bates, C. Cameron, and K. R. Smith, "Kerosene subsidies for household lighting in India: what are the impacts?," *Environmental Research Letters,* vol. 11, no. 4, pp. 044014, 2016.

[47] R. Gupta, A. Pandit, A. Nirjar, and P. Gupta, "Husk Power Systems: Bringing Light to Rural India and Tapping Fortune at the Bottom of the Pyramid," *Asian Journal of Management Cases,* vol. 10, no. 2, pp. 129-143, 2013.

[48] K. Ubilla, G. A. Jimenez-Estevez, R. Hernadez, L. Reyes-Chamorro, C. Hernandez Irigoyen, B. Severino, and R. Palma-Behnke, "Smart Microgrids as a

Solution for Rural Electrification: Ensuring Long-Term Sustainability Through Cadastre and Business Models," *IEEE Transactions on Sustainable Energy,* vol. 5, no. 4, pp. 1310-1318, 2014.

[49] *Energy for all: Viet Nam's success in increasing access to energy through rural electrification.,* Asian Development Bank, Mandaluyong City, Philippines, 2011.

[50] C. R. Monroy, and A. S. S. Hernández, "Main issues concerning the financing and sustainability of electrification projects in rural areas: international survey results," *Energy for Sustainable development,* vol. 9, no. 2, pp. 17-25, 2005.

[51] M. Dornan, "Access to electricity in Small Island Developing States of the Pacific: Issues and challenges," *Renewable and Sustainable Energy Reviews,* vol. 31, pp. 726-735, 2014.

[52] *NFPA 70: National Electrical Code*: National Fire Protection Association, 2011.

[53] A. Torkan, "Design, simulation and implementation of a high step-up z-source dc-dc converter with flyback and voltage multiplier," Texas A&M University, 2016.

[54] P. Fang Zheng, "Z-source inverter," *IEEE Transactions on Industry Applications,* vol. 39, no. 2, pp. 504-510, 2003.

[55] D. W. Hart, *Power electronics*: Tata McGraw-Hill Education, 2011.

[56] R. W. A. A. D. Doncker, D. M. Divan, and M. H. Kheraluwala, "A three-phase soft-switched high-power-density DC/DC converter for high-power applications," *IEEE Transactions on Industry Applications,* vol. 27, no. 1, pp. 63-73, 1991.

[57] Y. Arafat, L. B. Tjernberg, and S. Mangold, "Feasibility study on low voltage DC systems using smart meter data." pp. 1-4.

[58] S. A. L. S. N. Zealand, "Stand-alone power systems - System design," SAI Global Limited, 2010.

[59] "Surface meteorology and Solar Energy - A renewable energy resource web site."

[60] D. Elliott, C. Holladay, W. Barchet, H. Foote, and W. Sandusky, *Wind energy resource atlas of the United States*, vol. 87, 1987.

[61] T. Kapur, T. C. Kandpal, and H. P. Garg, "ELECTRICITY GENERATION FROM RICE HUSK IN INDIAN RICE MILLS: POTENTIAL AND FINANCIAL VIABILITY," *Biomass and Bioenergy*, vol. 10, no. 5/6, pp. 393-403, 1998.

[62] S. C. Bhattacharyya, "Viability of off-grid electricity supply using rice husk: A case study from South Asia," *Biomass and Bioenergy*, vol. 68, pp. 44-54, 2014.

[63] A. F. Santiaguel, "A second life for rice husks," *Rice Today*, vol. 12, no. 2, 2013.

[64] "Rice production doubles in Bihar, Jharkhand," *Times of India*, 2012.

[65] "DSP80-290P Panel Datasheet," https://www.enfsolar.com/pv/panel-datasheet/Polycrystalline/16727.

[66] B. O. Agajelu, O. G. Ekwueme, N. S. Obuka, and G. O. Ikwu, "Life cycle cost analysis of a diesel/photovoltaic hybrid power generating system," *Life*, vol. 3, no. 1, 2013.